

Washington University School of Medicine

Digital Commons@Becker

2020-Current year OA Pubs

Open Access Publications

1-1-2023

Multi-omic association study identifies DNA methylation-mediated genotype and smoking exposure effects on lung function in children living in urban settings

Matthew Dapas
University of Chicago

Michelle A. Gill
Washington University School of Medicine in St. Louis
et al

Follow this and additional works at: https://digitalcommons.wustl.edu/oa_4



Part of the [Medicine and Health Sciences Commons](#)

Please let us know how this document benefits you.

Recommended Citation

Dapas, Matthew; Gill, Michelle A.; and et al, "Multi-omic association study identifies DNA methylation-mediated genotype and smoking exposure effects on lung function in children living in urban settings." *PLoS Genetics*. 19, 1. e1010594 (2023).
https://digitalcommons.wustl.edu/oa_4/1216

This Open Access Publication is brought to you for free and open access by the Open Access Publications at Digital Commons@Becker. It has been accepted for inclusion in 2020-Current year OA Pubs by an authorized administrator of Digital Commons@Becker. For more information, please contact vanam@wustl.edu.

RESEARCH ARTICLE

Multi-omic association study identifies DNA methylation-mediated genotype and smoking exposure effects on lung function in children living in urban settings

Matthew Dapas^{1*}, Emma E. Thompson¹, William Wentworth-Sheilds¹, Selene Clay¹, Cynthia M. Visness², Agustin Calatroni², Joanne E. Sordillo³, Diane R. Gold^{4,5}, Robert A. Wood⁶, Melanie Makhija⁷, Gurjit K. Khurana Hershey^{8,9}, Michael G. Sherenian^{8,9}, Rebecca S. Gruchalla¹⁰, Michelle A. Gill¹¹, Andrew H. Liu¹², Haejin Kim¹³, Meyer Kattan¹⁴, Leonard B. Bacharier¹⁵, Deepa Rastogi¹⁶, Matthew C. Altman¹⁷, William W. Busse¹⁸, Patrice M. Becker¹⁹, Dan Nicolae²⁰, George T. O'Connor²¹, James E. Gern¹⁸, Daniel J. Jackson¹⁸, Carole Ober^{1*}



1 Department of Human Genetics, University of Chicago, Chicago Illinois, United States of America, **2** Rho Inc., Durham, North Carolina, United States of America, **3** Department of Population Medicine, Harvard Medical School, Boston, Massachusetts, United States of America, **4** Department of Environmental Health, Harvard T.H. Chan School of Public Health, Boston, Massachusetts, United States of America, **5** Channing Division of Network Medicine, Brigham and Women's Hospital, Harvard Medical School, Boston, Massachusetts, United States of America, **6** Department of Pediatrics, Johns Hopkins University Medical Center, Baltimore, Maryland, United States of America, **7** Division of Allergy and Immunology, Ann & Robert H. Lurie Children's Hospital, Chicago, Illinois, United States of America, **8** Department of Pediatrics, University of Cincinnati College of Medicine, Cincinnati, Ohio, United States of America, **9** Division of Asthma Research, Cincinnati Children's Hospital Medical Center, Cincinnati, Ohio, United States of America, **10** Department of Internal Medicine, University of Texas Southwestern Medical Center, Dallas, Texas, United States of America, **11** Department of Pediatrics, Washington University School of Medicine, St. Louis, Missouri, United States of America, **12** Department of Allergy and Immunology, Children's Hospital Colorado, University of Colorado School of Medicine, Aurora, Colorado, United States of America, **13** Department of Medicine, Henry Ford Health System, Detroit, Michigan, United States of America, **14** Columbia University College of Physicians and Surgeons, New York, New York, United States of America, **15** Monroe Carell Jr. Children's Hospital at Vanderbilt University Medical Center, Nashville, Tennessee, United States of America, **16** Children's National Health System, Washington, District of Columbia, United States of America, **17** Department of Allergy and Infectious Diseases, University of Washington, Seattle, Washington, United States of America, **18** Department of Pediatrics and Medicine, University of Wisconsin School of Medicine and Public Health, Madison, Wisconsin, United States of America, **19** National Institute of Allergy and Infectious Diseases, Bethesda, Maryland, United States of America, **20** Department of Statistics, University of Chicago, Chicago, Illinois, United States of America, **21** Pulmonary Center, Boston University School of Medicine, Boston, Massachusetts, United States of America

* mdapas@uchicago.edu (DM); c-ober@genetics.uchicago.edu (OC)

OPEN ACCESS

Citation: Dapas M, Thompson EE, Wentworth-Sheilds W, Clay S, Visness CM, Calatroni A, et al. (2023) Multi-omic association study identifies DNA methylation-mediated genotype and smoking exposure effects on lung function in children living in urban settings. *PLoS Genet* 19(1): e1010594. <https://doi.org/10.1371/journal.pgen.1010594>

Editor: Wei Pan, University of Minnesota School of Public Health, UNITED STATES

Received: June 6, 2022

Accepted: December 23, 2022

Published: January 13, 2023

Peer Review History: PLOS recognizes the benefits of transparency in the peer review process; therefore, we enable the publication of all of the content of peer review and author responses alongside final, published articles. The editorial history of this article is available here: <https://doi.org/10.1371/journal.pgen.1010594>

Copyright: This is an open access article, free of all copyright, and may be freely reproduced, distributed, transmitted, modified, built upon, or otherwise used by anyone for any lawful purpose. The work is made available under the [Creative Commons CC0](https://creativecommons.org/licenses/by/4.0/) public domain dedication.

Data Availability Statement: Phenotype, genotype, GWAS summary statistics, and whole-genome sequencing files are available in dbGaP

Abstract

Impaired lung function in early life is associated with the subsequent development of chronic respiratory disease. Most genetic associations with lung function have been identified in adults of European descent and therefore may not represent those most relevant to pediatric populations and populations of different ancestries. In this study, we performed genome-wide association analyses of lung function in a multiethnic cohort of children ($n = 1,035$) living in low-income urban neighborhoods. We identified one novel locus at the *TDRD9* gene in chromosome 14q32.33 associated with percent predicted forced expiratory volume in one

under accession phs002921.v1.p1. The URECA gene expression data are available on the Gene Expression Omnibus (GEO) under accession numbers GSE145505 (NECs) and GSE96783 (PBMcs). The URECA DNA methylation data are available in GEO under the reference series GSE217337. The pCHI-C data are available in GEO under the reference series GSE152550.

Funding: This work was supported by NIH grants U19 AI62310, HHSN272200900052C, HHSN272201000052I, UM1 AI114271, UG3 OD023282, and UM1 AI160040. Site data collection was supported by the following NIH grants: RR00052, UL1 TR001079 (Baltimore); M01 RR00533, UL1 RR025771, 1 UL1 TR001430 (Boston); UL1 TR000150 (Chicago); UL1 TR000451, UL1 TR001105 (Dallas); UI1 RR025780 (Denver); UL1 TR000040, M01 RR00071, UL1 RR024156 (New York); UL1 TR000075 (D.C.); UL1 TR000077 (Cincinnati). M. D. was supported by TL1 TR002388 and T32 HL007605.

Competing interests: All authors, with the exception of M. Altman and P. Becker, report grants from NIH/NIAID during the conduct of study. M. Dapas, C. Visness, A. Calatroni and P. Becker have nothing to disclose outside the submitted work. C. Ober reports personal fees from American Association of Asthma, Allergy and Immunology, outside the submitted work. M. Altman reports personal fees from Sanofi-Regeneron outside the submitted work. W. Busse reports personal fees from Boston Scientific, Novartis, GlaxoSmithKline, Genentech, Sanofi/Genzyme, AstraZeneca, Teva, Regeneron and Elsevier outside the submitted work. M. Gill reports an honorarium for and support for travel to the 2017 AAAAI meeting during the conduct of study and monetary compensation from the American Academy of Pediatrics for her work teaching the biannual Pediatrics board review course, PREP The Course. K. Hershey reports grants from Adare, during the conduct of the study. D. Jackson reports personal fees from Novartis, Boehringer Ingelheim, Pfizer, Regeneron, AstraZeneca, Sanofi and Vifor Pharma, grants and personal fees from GlaxoSmithKline and grants from NIH/NHLBI, outside the submitted work. M. Kattan reports personal fees from Regeneron, outside the submitted work. R. Gruchalla reports government employment from Center for Biologics Evaluation and Research as well as personal fees from Consulting Massachusetts Medical Society, outside the submitted work. A. Liu reports personal fees from Phadia ThermoFisher as consulting honoraria, grants and non-financial support from

second (FEV₁) ($p = 2.4 \times 10^{-9}$; $\beta_z = -0.31$, 95% CI = -0.41– -0.21). Mendelian randomization and mediation analyses revealed that this genetic effect on FEV₁ was partially mediated by DNA methylation levels at this locus in airway epithelial cells, which were also associated with environmental tobacco smoke exposure ($p = 0.015$). Promoter-enhancer interactions in airway epithelial cells revealed chromatin interaction loops between FEV₁-associated variants in *TDRD9* and the promoter region of the *PPP1R13B* gene, a stimulator of p53-mediated apoptosis. Expression of *PPP1R13B* in airway epithelial cells was significantly associated the FEV₁ risk alleles ($p = 1.3 \times 10^{-5}$; $\beta = 0.12$, 95% CI = 0.06–0.17). These combined results highlight a potential novel mechanism for reduced lung function in urban youth resulting from both genetics and smoking exposure.

Author summary

Lung function is determined by both genetic and environmental factors. Impairment of lung function can result from harmful environmental exposures in early life, which disproportionately affect children living in low-income, urban communities. However, most genetic association studies of lung function have been performed in adults and without regard for socioeconomic status. Therefore, genetic risk factors discovered to date may not reflect those most relevant to high-risk populations. In this study, we sought to identify genetic variants correlated with lung function in a multiethnic cohort of children living in low-income, urban neighborhoods and analyze how tobacco smoke exposure may influence any genetic effects. We discovered a common genetic variant associated with lower lung function in this population, and we found that the association was mediated by nearby epigenetic changes in DNA methylation, which were in turn correlated with smoking exposure. We then identified a nearby gene, *PPP1R13B*, which is known to aid in the deactivation of damaged cells, whose expression in airway cells aligned with these genetic and epigenetic effects. This study reveals a potential mechanism through which genetic risk and environmental exposures can affect airway development, perhaps leading to interventions that can help reduce the burden of asthma in socioeconomically disadvantaged children.

Introduction

Reduced lung function is a hallmark of asthma and chronic obstructive pulmonary disease (COPD). Lung function measures, such as forced expiratory volume in one second (FEV₁) and forced vital capacity (FVC), are strong predictors of future all-cause mortality [1–6]. Airway obstruction often begins in early life [7–10], with lower lung function in infancy being a risk factor for the development of asthma in childhood [11] and COPD in late adulthood [12].

Genetic factors contribute to differences in lung function among individuals, with heritability estimates ranging from 0.50 for FEV₁ to 0.66 for FEV₁/FVC ratio [13]. The many genome-wide association studies (GWAS) of lung function measures [14–25] have implicated pathways related to lung development [20,26–28], inflammation [26], and tissue repair [29], among others [29]. Lung function is also affected by environmental exposures, such as smoking [30–32] and air pollution [33], which can disrupt airway development in early life, increasing the risk of childhood asthma and perhaps other chronic obstructive diseases [8–12,34,35]. For

ResMed/Propeller Health, non-financial support from Revenio, grants and personal fees from Avillion and personal fees from Labcorp, outside the submitted work. L. Bacharier reports personal fees from GlaxoSmithKline, Genentech/Novartis, DBV Technologies, Teva, Boehringer Ingelheim, AstraZeneca, WebMD/Medscape, Sanofi/Regeneron, Vectura and geCircassia and personal fees and non-financial support from Merckoutside the submitted work. J. Gern reports personal fees from AstraZeneca and Gossamer Bio and personal fees and stock options from Meissa Vaccines Inc, outside the submitted work. In addition, Dr. Gern has a patent Methods of Propagating Rhinovirus C in Previously Unsusceptible Cell Lines issued, and a patent Adapted Rhinovirus C issued. G. O'Connor reports personal fees from AstraZeneca and grants from Janssen Pharmaceuticals, outside the submitted work. R. Wood reports grants from DBV, Aimmune, Astellas, HAL-Allergy and Regeneron and royalties from Up to Date, outside the submitted work. Dr. Becker's co-authorship of this publication does not necessarily constitute endorsement by the National Institute of Allergy and Infectious Diseases, the National Institutes of Health or any other agency of the United States government.

example, exposure to second hand smoke in utero and through childhood is associated with increased risk of childhood asthma [36], lower lung function in adolescence [37], and larger declines in lung function later in life [38,39]. Such adverse exposures are known to alter the epigenetic landscape in exposed individuals [40,41], potentially mediating downstream biological effects [42–44] and modifying genetic associations with lung function [45,46].

Environmental risk factors disproportionately affect socioeconomically disadvantaged children, particularly those living in urban environments [47,48]. In fact, socioeconomic effects contribute to disparities in lung health [49], including the higher burden of chronic respiratory disease among Black and Hispanic children compared to non-Hispanic white children [49–52]. Most genetic association studies of lung function, however, have been limited to adults of European descent. Therefore, genetic risk factors discovered to date may not reflect those most relevant to high-risk populations, which can further exacerbate health disparities [53,54]. Identifying genetic variants and epigenetic variation associated with lung function in high-risk, multiethnic, pediatric populations may provide more direct insights into the early development of impaired lung function.

In this study, we analyzed measures of lung function from the Asthma Phenotypes in the Inner City (APIC) [55,56] and Urban Environment and Childhood Asthma (URECA) cohorts [57], which consist of children living in low-income neighborhoods in 10 U.S. cities. We performed whole-genome sequencing (WGS) on 1,035 participants from APIC and URECA (ages 5–17 years; 67% non-Hispanic Black, 25% Hispanic; 66% with doctor-diagnosed asthma) and performed a GWAS with FEV₁ and the FEV₁/FVC ratio. We then performed expression quantitative trait locus (eQTL) and methylation quantitative trait locus (meQTL) mapping in airway epithelial cells and peripheral blood mononuclear cells (PBMCs) from a subset of the URECA children. We further tested for genotype and DNA methylation interactions with smoking exposure. We aimed to identify methylation-mediated genetic and smoking exposure associations with lung function, linking environmental effects, epigenetic modifications, and specific genetic risk alleles to reduced pulmonary health in urban youth.

Results

Genetic variants at the *TDRD9* locus are associated with lung function

We completed WGS and variant calling on 1,035 participants from the APIC and URECA studies (APIC = 508, URECA = 527; Table 1). The mean sequencing depth was 31.6x per sample (S1A Fig). On average, 95.3%, 90.3% and 62.6% of each genome was mapped with at least 10x, 20x and 30x sequencing read depth, respectively (S1B Fig). Approximately 3.8 million high-confidence autosomal variants were called per sample. Variant call concordance between replicate sample pairs (n = 3) was >99.9% for single nucleotide polymorphisms (SNPs) and was 98.9% for insertions and deletions (InDels; S1 Table).

The sequenced cohort included 696 (67%) participants who self-identified as non-Hispanic Black and 258 (25%) who self-identified as Hispanic (Table 1). Principal component and admixture analyses using genotypes were conducted to characterize the ancestry of the participants (Fig 1). This revealed that the genetic ancestry of our sample was 66% African, 26% European, 7% Native American, and 1% East Asian. The cohort was 54% male and included 681 (66%) children diagnosed with asthma (Table 1).

Using the WGS variant calls for 14.1 million variants with minor allele frequency (MAF) ≥ 0.01 , we performed a GWAS of two lung function traits: FEV₁ (% predicted) and FEV₁/FVC (Z-scores), measured between ages 5–17 (Table 1, S2 Fig), adjusting for age, sex, asthma diagnosis, the first 10 principal components (PCs) of ancestry, and sample relatedness using a

Table 1. Demographic characteristics of sequenced APIC and URECA participants.

Characteristic	All	APIC	URECA
Number	1035	508	527
Age, years, mean (SD)	10.3 (2.5)	10.9 (3.1)	9.6 (1.1)
Female sex	477 (46%)	216 (43%)	261 (50%)
<i>Race/Ethnicity</i>			
Black (non-Hispanic)	696 (67%)	319 (63%)	377 (72%)
White (non-Hispanic)	14 (1%)	7 (1%)	7 (1%)
Hispanic	258 (25%)	153 (30%)	105 (20%)
Other/mixed	64 (6%)	26 (5%)	38 (7%)
Unknown	3 (<1%)	2 (<1%)	1 (<1%)
<i>Site</i>			
Baltimore	234 (23%)	85 (17%)	149 (28%)
Boston	189 (18%)	65 (13%)	124 (23%)
Chicago	62 (6%)	62 (12%)	-
Cincinnati	45 (4%)	45 (9%)	-
Dallas	38 (4%)	38 (9%)	-
Denver	59 (6%)	59 (12%)	-
Detroit	50 (5%)	50 (10%)	-
New York	164 (16%)	64 (13%)	100 (19%)
St. Louis	155 (15%)	-	155 (29%)
Washington, D.C.	39 (4%)	39 (8%)	-
Household income < \$15k	550 (54%)	273 (54%)	277 (54%)
Caretaker completed HS	756 (73%)	364 (72%)	392 (74%)
Caretaker smokes*	315 (33%)	123 (27%)	192 (39%)
Asthma	681 (75%)	508 (100%)	173 (43%)
BMI, Z-score, mean (SD)	0.9 (1.2)	1.0 (1.2)	0.8 (1.1)
FEV ₁ , % predicted, mean (SD)	94.9 (16.3)	91.9 (17.6)	98.5 (14.5)
FEV ₁ /FVC, mean (SD)	0.80 (0.09)	0.78 (0.10)	0.83 (0.07)

Results are presented as counts and percentages or as means with standard deviations. Missing data were not included in percentage calculations. Ages for URECA correspond to the year the genome-wide association study lung function data were collected.

*Caretaker smoking status in URECA was collected at age 10. APIC: Asthma Phenotypes in the Inner City; BMI: body mass index; FEV₁: forced expiratory volume in one second; FEV₁/FVC: ratio of FEV₁ to forced vital capacity; HS: high school; URECA: Urban Environment and Childhood Asthma.

<https://doi.org/10.1371/journal.pgen.1010594.t001>

linear mixed model [58]. The FEV₁ GWAS included 896 participants from APIC (n = 504) and URECA (n = 392), and the FEV₁/FVC GWAS included 886 participants from APIC (n = 497) and URECA (n = 389). The genomic control factor, λ_{GC} , for both GWAS results was 1.02 (S3 Fig), indicating adequate control for population stratification. We identified one locus on chromosome 14q32.33 that was associated with FEV₁ at genome-wide significance ($p < 2.5 \times 10^{-8}$); no other variants were associated with FEV₁ and no variants were associated with FEV₁/FVC at genome-wide levels of significance (Fig 2). The FEV₁ locus on chromosome 14 consisted of a 200 kb region of associated variants in high linkage disequilibrium (LD) across the *TDRD9* (Tudor Domain Containing 9) gene (Fig 3, S2 Table). The minor allele at the lead SNP (rs10220464; MAF = 0.30) was significantly associated with lower FEV₁ ($p = 2.4 \times 10^{-9}$; $\beta_z = -0.31$, 95% confidence interval (CI) = -0.41 - -0.21) and nominally associated

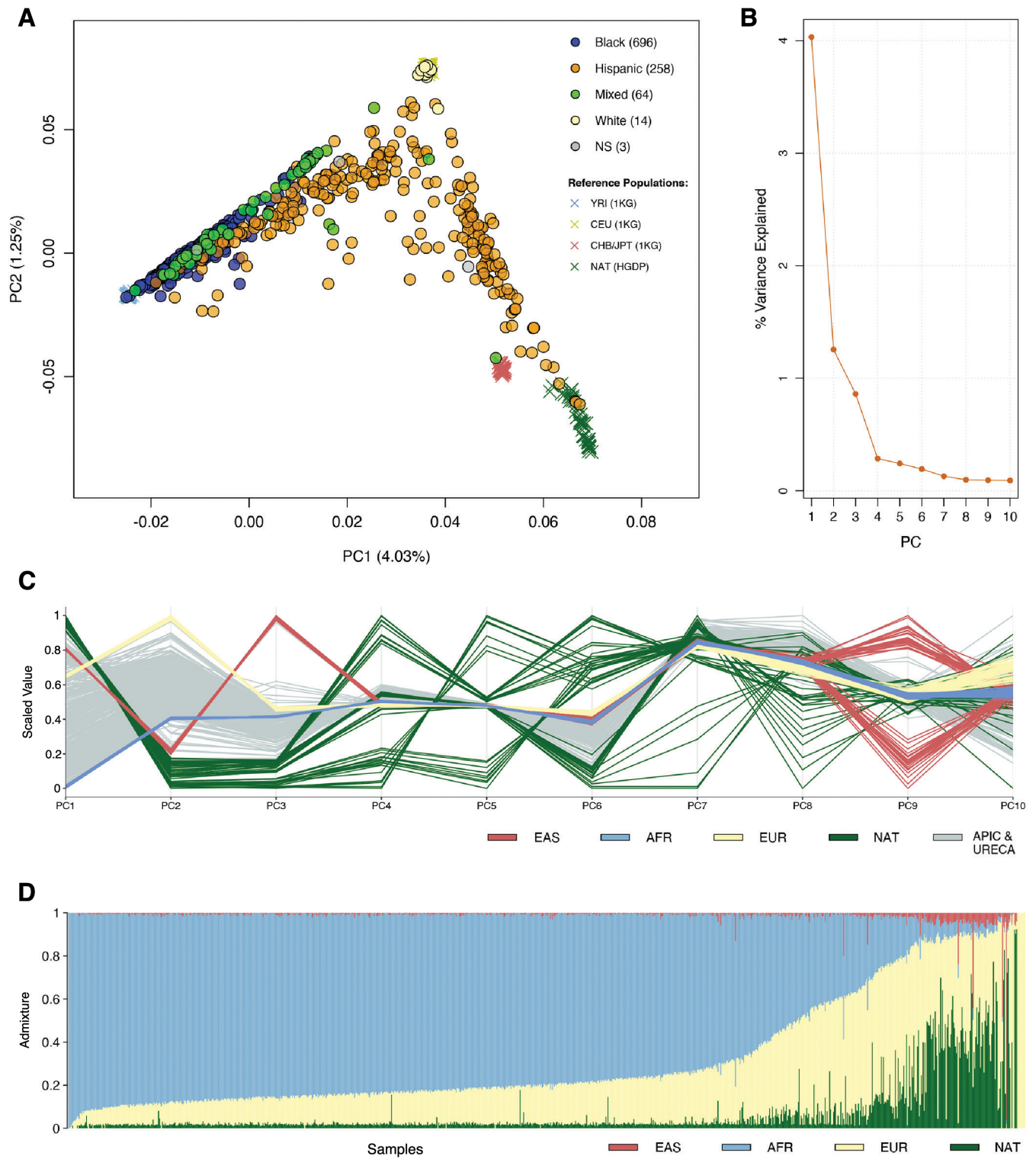


Fig 1. Ancestry composition of sequenced APIC & URECA participants. A) The top two principal components (PCs) of ancestry are plotted for sequenced APIC & URECA participants, colored by self-identified race/ethnicity, along with the four ancestry reference populations used for determining ancestry. NS = not specified. B) The proportion of genetic variance explained by each of the top 10 PCs. C) The relative values of the top 10 PCs are plotted for each sample, colored by reference population. D) The estimated proportion of admixture from each ancestral population is shown for each sequenced APIC & URECA participant. Each vertical line corresponds to one sample. 1KG, 1000 Genomes project; HGDP, Human Genome Diversity Project; YRI, Yoruba in Ibadan, Nigeria; CEU, Utah residents with Northern and Western European ancestry; CHB, Han Chinese in Beijing, China; JPT, Japanese in Tokyo, Japan; NAT, Native Americans from HGDP; EAS, East Asian ancestry; AFR, African ancestry; EUR, European ancestry.

<https://doi.org/10.1371/journal.pgen.1010594.g001>

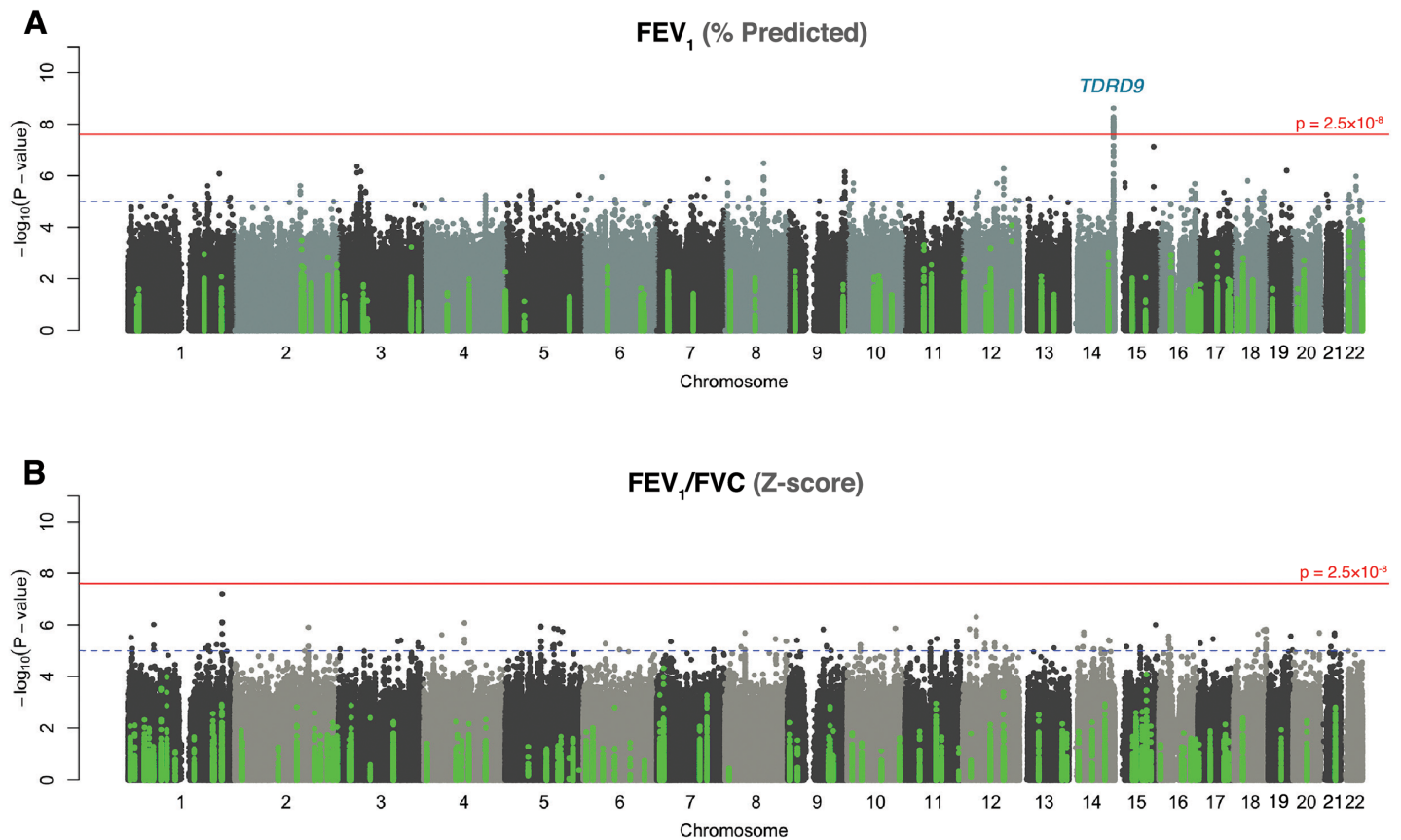


Fig 2. Genome-wide association results. GWAS Manhattan plots for **A)** FEV₁ and **B)** FEV₁/FVC ratio. The horizontal red line indicates genome-wide significance ($p \leq 2.5 \times 10^{-8}$). The dotted horizontal blue line indicates $p = 1 \times 10^{-5}$. Variants colored in green are in previously identified GWAS loci [23]. FEV₁, forced expiratory volume in one second; FEV₁/FVC, ratio of FEV₁ to forced vital capacity.

<https://doi.org/10.1371/journal.pgen.1010594.g002>

with lower FEV₁/FVC ($p = 1.1 \times 10^{-3}$; $\beta_z = -0.17$, 95% CI = -0.28 - -0.07). Fine-mapping analysis at this locus (chr14:103.7–104.3Mb) revealed one 95% credible set of effect variables consisting of 59 SNPs, with rs10220464 having the highest individual posterior inclusion probability among them (S4 Fig). We did not detect any significant differences in rs10220464 association effect size by ancestry or asthma status or study for FEV₁ (Fig 4). Furthermore, the *TDRD9* locus remained the only genome-wide significant association when the two GWAS were performed without adjustment for asthma status (S5 Fig). The overall effect size correlations between asthma-adjusted and unadjusted GWAS results were $r = 0.981$ for FEV₁ and $r = 0.954$ for FEV₁/FVC.

We examined association results for the previously identified FEV₁ and FEV₁/FVC loci reported in the meta-analysis of the UK Biobank and SpiroMeta Consortium by Shrine and colleagues ($n = 400,102$) [23], which included 70 loci for FEV₁ and 117 for FEV₁/FVC. Of these, 64 of the lead SNPs for FEV₁ and 112 for FEV₁/FVC were genotyped in the APIC and URECA sample. Only one SNP, for FEV₁, replicated with false discovery rate (FDR) $q < 0.05$ (rs9610955; $p = 1.0 \times 10^{-4}$; $\beta_z = -0.38$, 95% CI = -0.58 - -0.19; S6 and S7 Figs). Cumulatively, 56% ($n = 36$) and 54% ($n = 60$) of these SNPs demonstrated consistent directions of effect for FEV₁ and FEV₁/FVC, respectively, with effect size correlations of 0.29 (95% CI = 0.05–0.50; $p = 0.020$) for FEV₁ and 0.42 (95% CI = 0.25–0.56; $p = 4.2 \times 10^{-6}$) for FEV₁/FVC.

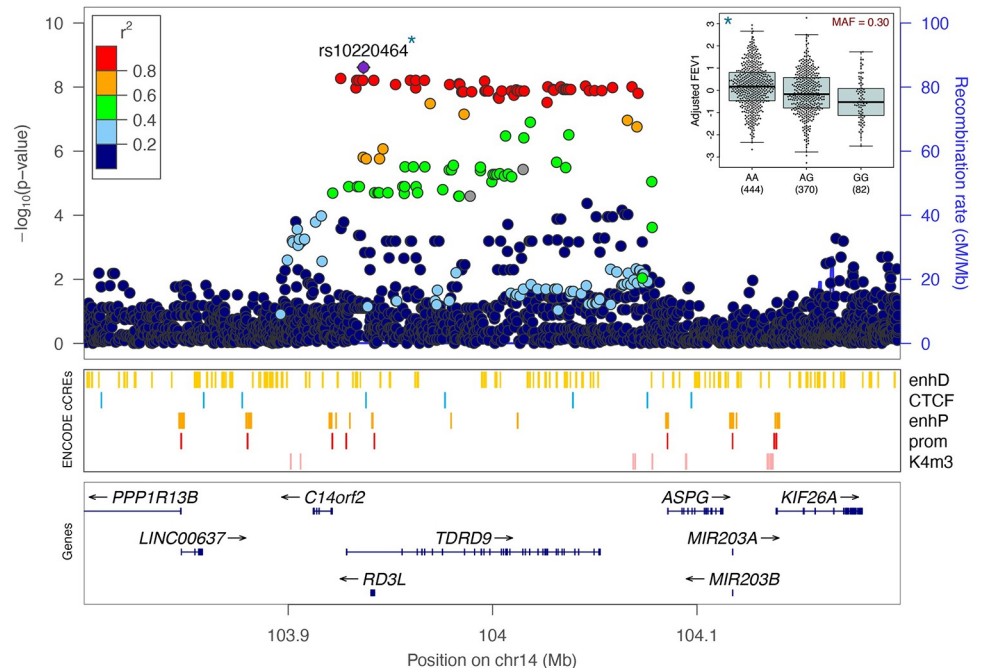


Fig 3. FEV₁-associated variants on chromosome 14q32.33. FEV₁ association results are shown at the *TDRD9* gene locus. Each variant is plotted according to its position and $-\log_{10}$ p-value, colored by linkage disequilibrium to the lead variant, rs10220464, within the sample. Candidate cis-Regulatory Elements (cCREs) from ENCODE [59] are also shown for the region. The inset panel in the upper right shows the distribution of adjusted FEV₁ values by rs10220464 genotype. FEV₁, forced expiratory volume in one second; MAF, minor allele frequency; EnhD, distal enhancer-like signature; CTCF, CCCTC-binding factor sites; enhP, proximal enhancer-like signature; prom, promoter-like signature; K4m3, trimethylation of histone H3 at lysine 4.

<https://doi.org/10.1371/journal.pgen.1010594.g003>

Lung function risk alleles are associated with DNA methylation at the *TDRD9* locus in airway epithelial cells

The majority of complex trait-associated variants exert effects by altering gene regulatory networks [60–62]. These changes are often marked by quantitative differences in DNA methylation levels [63–65]. We therefore investigated correlations between the FEV₁-associated allele at *TDRD9* and DNA methylation at the locus in upper airway (nasal) epithelial cells (NECs) from URECA children at age 11 ($n = 286$). We tested for associations between the FEV₁ genotype, as tagged by rs10220464, and DNA methylation levels at 796 CpG sites within 10 kb of any *TDRD9* locus variants associated with FEV₁ at $p < 1 \times 10^{-5}$ ($n = 82$ variants). The rs10220464 genotype was an meQTL for 5 CpG sites at an FDR < 0.05 (S3 Table). DNA methylation levels at only one of these CpG sites, cg03306306 ($p = 2.3 \times 10^{-4}$; $\beta = 0.07$, 95% CI = 0.03–0.10; Fig 5A), was also significantly associated with FEV₁ at age 10 in URECA ($p = 0.011$; $\beta = -11.48$, 95% CI = -20.27–-2.69; Fig 5B). The rs10220464 genotype accounted for 4.7% of residual variation in cg03306306 methylation, and cg03306306 methylation explained 2.4% of residual variation in FEV₁.

We then analyzed cg03306306 methylation in PBMCs collected at age 7 ($n = 169$) [66] from URECA children to evaluate whether the genotype and lung function associations observed in NECs were shared with blood cells. In PBMCs, we observed no correlation between the rs10220464 risk allele and cg03306306 methylation (Fig 5C), nor was there an association between cg03306306 methylation and FEV₁ (Fig 5D). These results indicate that cg03306306 methylation dynamics in the airway epithelium are not present in peripheral blood cells.

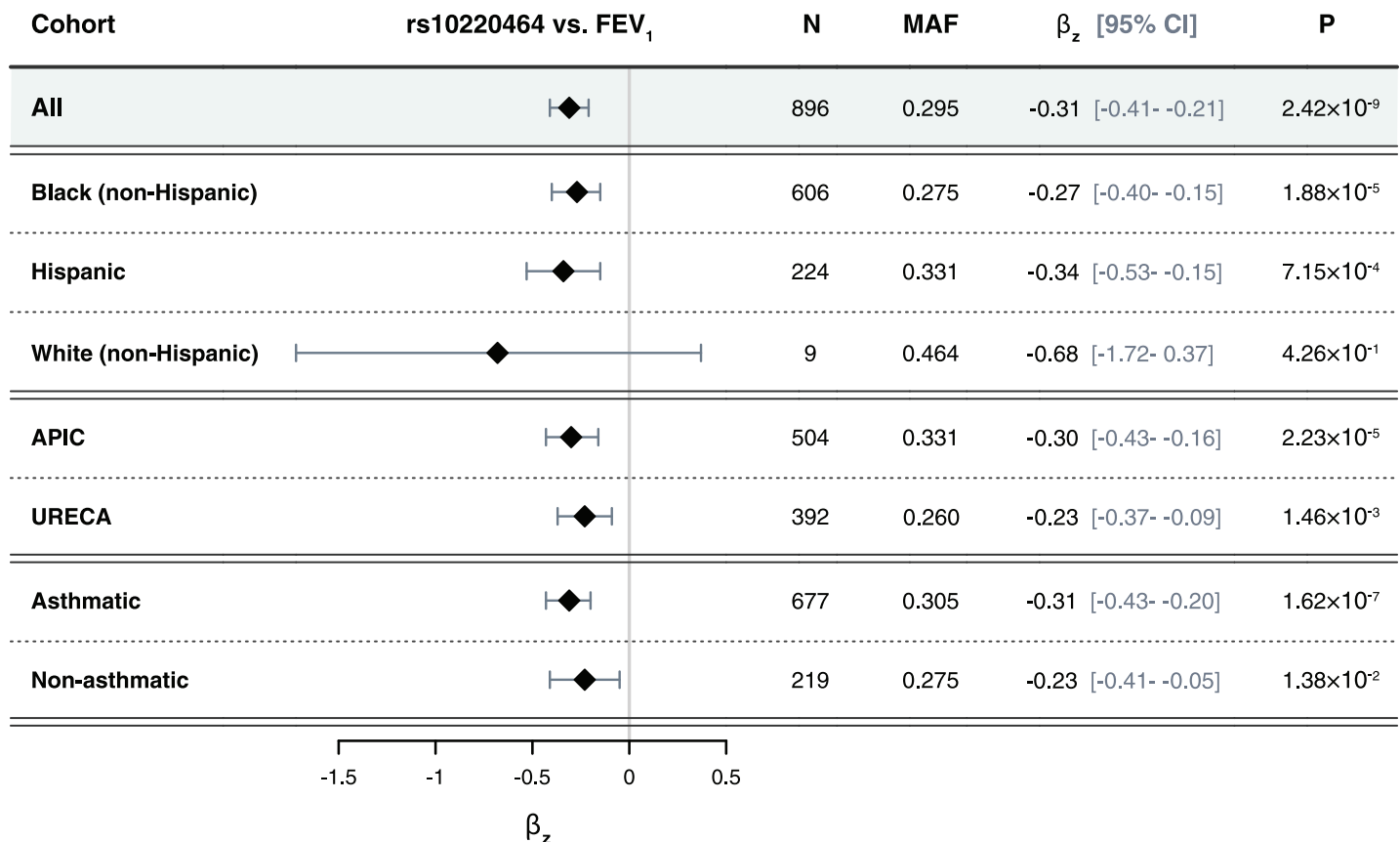


Fig 4. Rs10220464 effect size heterogeneity. A forest plot of the associations between rs10220464 and FEV₁ (% predicted) are shown for distinct sub-cohorts distinguished by self-identified race/ethnicity, study, and asthma status. β_z , the association effect size between the rs10220464 allele count and the adjusted and normalized FEV₁ (% predicted) values; FEV₁, forced expiratory volume in one second; N, total number of individuals included in the association test; MAF, minor allele frequency within the sub-cohort; P, the association p-value.

<https://doi.org/10.1371/journal.pgen.1010594.g004>

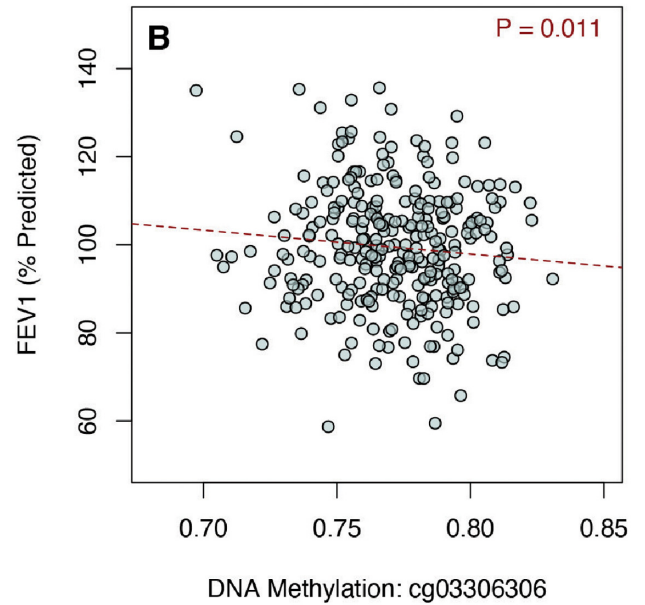
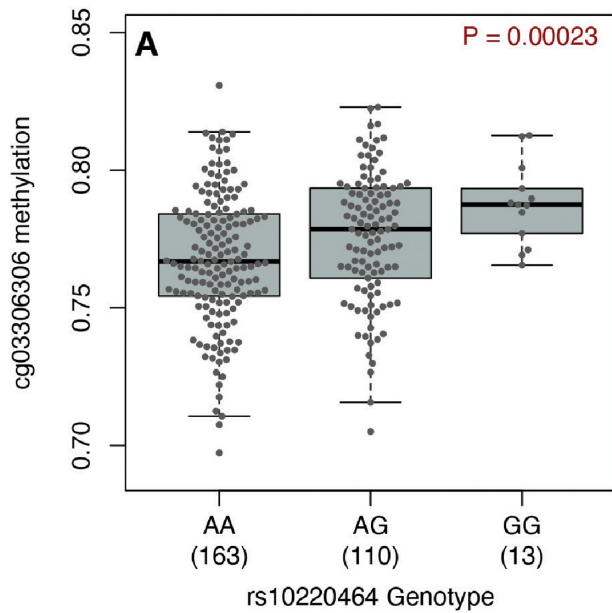
Smoking exposure is associated with DNA methylation at the *TDRD9* locus

DNA methylation at the *TDRD9* locus had previously been associated with maternal smoking during pregnancy [67,68]. Therefore, we tested for associations between environmental tobacco smoke exposure (S8 Fig) and DNA methylation at this locus in the URECA children. Methylation at cg03306306 in NECs was significantly associated with nicotine metabolite (cotinine) levels in urine collected at ages 7–10 years ($p = 0.015$; $\beta = 0.03$, 95% CI = 0.01–0.05; Fig 6).

Methylation at cg03306306 in PBMCs from age 7 was not associated with urine cotinine levels.

To determine if there was an interaction effect between genotype and smoking exposure on DNA methylation and/or lung function, we repeated the cotinine association tests in URECA with the addition of an interaction term to assess if the genotype effect differed between individuals with low and high exposures to smoking. There were no significant genotype-by-smoking exposure interaction effects on methylation levels in NECs or PBMCs in URECA, nor were there any significant methylation-by-smoking effects on FEV₁ (S9 Fig). There was modest evidence for a genotype-by-smoking exposure interaction effect on FEV₁ in the combined APIC and URECA sample, but this did not reach statistical significance ($p = 0.06$, S10 Fig). Considering the ages of the participants in APIC and URECA, most tobacco exposures were likely due to secondhand smoke.

NECs



PBMCs

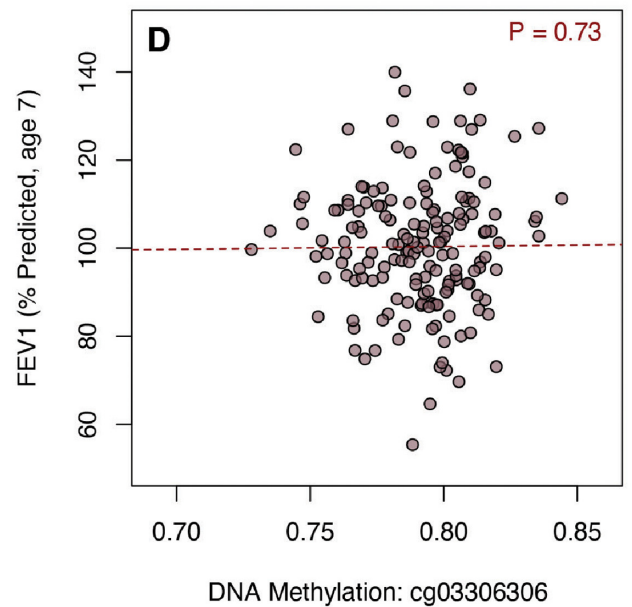
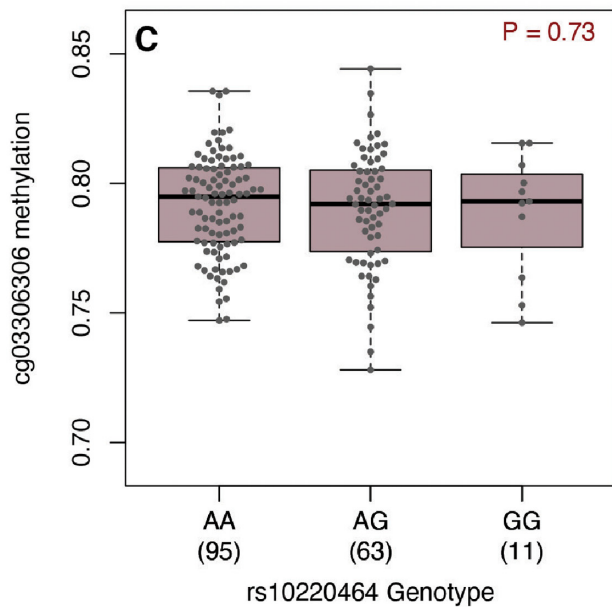


Fig 5. Genotype and FEV₁ associations with DNA methylation. DNA methylation levels at cg03306306 are shown by rs10220464 genotype and FEV₁ measures are plotted against cg03306306 methylation levels in NECs at age 11 (A, B), and PBMCs at age 7 (C, D) from URECA. FEV₁, forced expiratory volume in one second; NECs, nasal epithelial cells; PBMCs, peripheral blood mononuclear cells; URECA, Urban Environment and Childhood Asthma study.

<https://doi.org/10.1371/journal.pgen.1010594.g005>

Genetic effects on lung function are mediated by DNA methylation

To determine if DNA methylation at the *TDRD9* locus had a causal effect on lung function, we performed a Mendelian randomization analysis using two-stage least squares (2SLS)

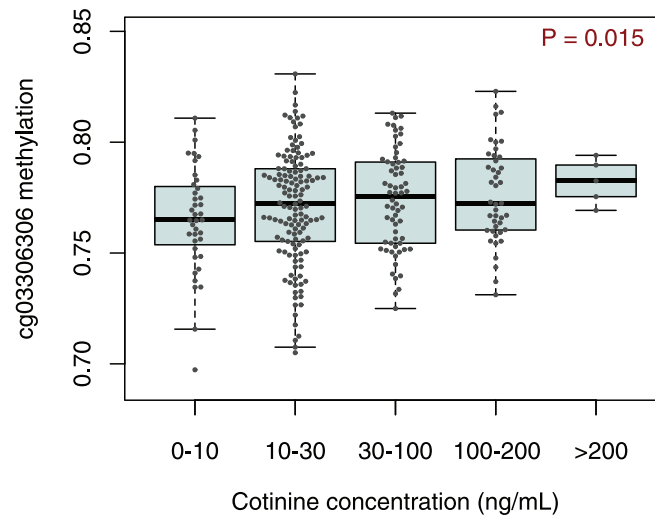


Fig 6. DNA methylation association with smoking exposure. DNA methylation at cg03306306 in nasal epithelial cells at age 11 are plotted against urine cotinine levels from URECA at ages 8–10 as measured using the NicAlert assay ($n = 285$). URECA, Urban Environment and Childhood Asthma study.

<https://doi.org/10.1371/journal.pgen.1010594.g006>

regression. In the first stage, cg03306306 methylation levels in NECs were regressed on an instrument composed of four meQTLs for cg03306306 (rs11160777, rs137961671, rs7143936, rs11160776; [Materials and methods](#)). In the second stage, FEV₁ was regressed on the predicted DNA methylation values generated from the first stage regression, thereby yielding a causal effect estimate of cg03306306 methylation on FEV₁. Urine cotinine levels were included as a covariate in both stages. The variance explained in the first stage regression was $r^2 = 0.11$. The causal effect of cg03306306 methylation on FEV₁ was statistically significant ($p = 0.020$). We also tested a single, unweighted allele score of the instrumental variables and observed a causal effect association of $p = 0.045$ (stage-one $r^2 = 0.10$). We further performed a bootstrapped mediation analysis to test whether the rs10220464 risk allele effect on FEV₁ was mediated by DNA methylation. The indirect effect of rs10220464 on FEV₁ via cg03306306 methylation was significant, both when including asthma as a covariate ($\beta_z = -0.04$, 95% CI = -0.10– -0.003, percent mediated = 14.4%) and when asthma was not considered ($\beta_z = -0.04$, 95% CI = -0.10– -0.002, percent mediated = 15.0%). These results indicate that the effect of the FEV₁-associated genotype at the *TDRD9* locus is partially mediated through its impact on nearby DNA methylation levels.

Gene expression and promoter-enhancer interactions implicate *PPP1R13B*

Trait-associated variants and DNA methylation often affect the transcriptome by influencing the expression of one or more neighboring genes [69,70]. Identifying these correlations can help infer causal mechanisms [71]. Therefore, we next explored the relationship between the genotype for the lead FEV₁ variant rs10220464 and the expression of genes within 1 Mb in NECs and PBMCs from URECA children. Notably, the rs10220464 genotype was not associated with *TDRD9* expression levels in these cells (NECs: $p = 0.60$, $\beta = 0.12$; PBMCs: $p = 0.91$, $\beta = 0.014$). Of the 27 genes that were evaluated ([S4 Table](#)), rs10220464 was significantly associated with the expression of only one gene, *PPP1R13B* (Protein Phosphatase 1 Regulatory Subunit 13B; FDR $q = 2.77 \times 10^{-4}$; $p = 1.3 \times 10^{-5}$; $\beta = 0.12$, 95% CI = 0.06–0.17; [Fig 7A](#)), in NECs. *PPP1R13B* expression levels were also the most strongly associated of the 27 genes with

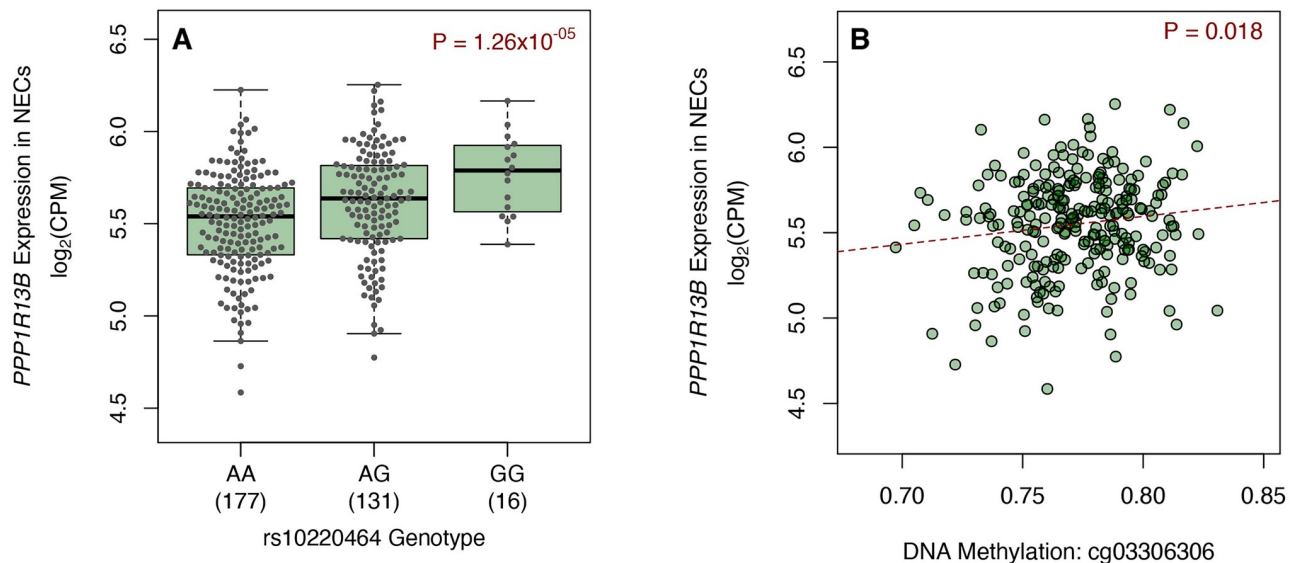


Fig 7. *PPP1R13B* gene expression in NECs. *PPP1R13B* gene expression in NECs at age 11 are plotted against A) rs10220464 genotype (n = 324) and B) DNA methylation at cg03306306 in NECs at age 11 (n = 254). NECs, nasal epithelial cells; CPM, counts per million.

<https://doi.org/10.1371/journal.pgen.1010594.g007>

methylation at cg03306306 in NECs ($p = 0.018$; $\beta = 0.10$, 95% CI = 0.02–0.18; Fig 7B).

PPP1R13B expression in NECs, however, was not associated with FEV₁ or smoking exposure (S11 Fig).

The transcription start site of *PPP1R13B* resides 87 kb from rs10220464 and 152 kb from cg03306306, suggesting long-range interactions between the FEV₁-associated genotype and the promoter of *PPP1R13B*. To determine whether any of the FEV₁-associated GWAS variants at the *TDRD9* locus resided in regions that physically interacted with the promoters of *cis*-genes, we evaluated chromatin interactions in lower airway (bronchial) epithelial cells (BECs) [72], assessed by promoter-capture Hi-C. Forty-two of the GWAS variants resided in regions that interacted with the promoters of 9 different genes expressed in NECs (Fig 8; S5 Table). The gene most frequently mapped to these variants was *PPP1R13B*, with 15 variants located in 3 different interaction loops. Moreover, the strongest observed interaction was between a region containing 4 FEV₁-associated variants and the *PPP1R13B* promoter (CHiCAGO score = 9.38; S5 Table), suggesting that this region is an enhancer for *PPP1R13B* expression. This putative enhancer region is located just 2.21 kb from cg03306306.

Summary of study associations

The associations between the *TDRD9* risk allele, cg03306306 DNA methylation in NECs, smoking exposure, *PPP1R13B* gene expression, and FEV₁ (% predicted) reported in this study are summarized in Fig 9.

Discussion

Using whole-genome sequence variant calls in an asthma-enriched cohort of predominantly African-American children raised in urban environments, we identified a genotype at the *TDRD9* locus associated with lower FEV₁% predicted. This genotype effect was partially mediated by DNA methylation in airway epithelial cells, which were also correlated with smoking exposure. Data from RNA-sequencing and promoter-capture Hi-C in airway epithelial cells

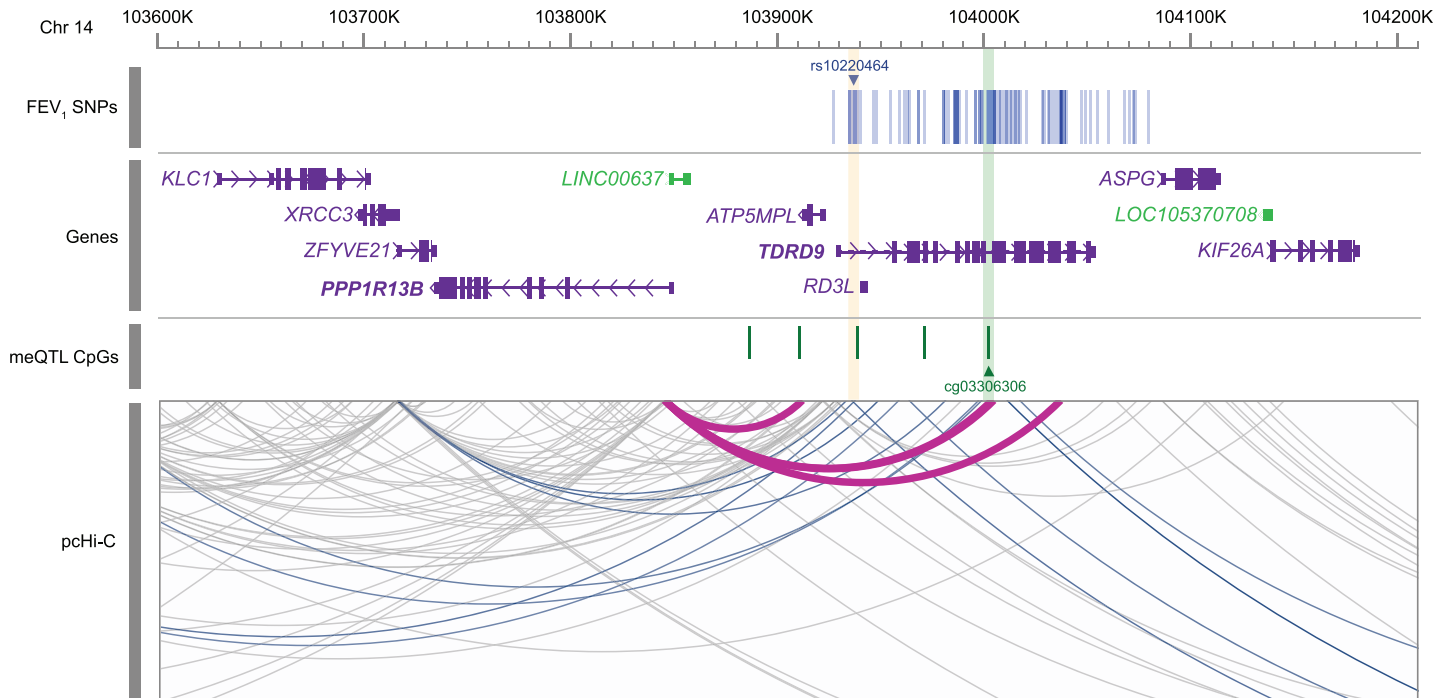


Fig 8. Promoter-enhancer interactions at *TDRD9* locus in nasal epithelial cells. Promoter-to-enhancer chromatin interactions captured by Hi-C in nasal epithelial cells from URECA at age 11 are displayed as grey arcs. SNPs associated with FEV₁ ($p < 1 \times 10^{-5}$) are marked by blue lines in the top row according to their genomic position on chromosome 14. The lead FEV₁ SNP, rs1022464, is highlighted in yellow. CpG sites associated with rs1022464 ($FDR < 0.05$) are displayed as green markers below the genes, with cg03306306 highlighted in green. Chromatin Interactions containing SNPs associated with FEV₁ ($p < 1 \times 10^{-5}$) are highlighted in blue. Magenta arcs highlight interactions between the *PPP1R13B* promoter and regions containing FEV₁ SNPs and/or rs1022464-associated CpG sites. FEV₁, forced expiratory volume in one second; SNPs, single nucleotide polymorphisms; meQTL, methylation quantitative trait locus; pcHi-C, promoter capture Hi-C.

<https://doi.org/10.1371/journal.pgen.1010594.g008>

suggested that these FEV₁-associated genetic and epigenetic variations influence the expression of the *PPP1R13B* gene through long-range interactions.

The *PPP1R13B* gene encodes a protein that promotes apoptosis, a form of programmed cell death, via its interaction with the tumor suppressor p53 and is often referred to by its alias ASPP1 (apoptosis-stimulating protein of p53 1) [73]. In response to oncogenic stress, PPP1R13B translocates to the nucleus, where it enhances the transcriptional activity of p53 on specific target genes relevant to apoptosis [74,75]. Exposure to smoking and fine particulate matter induces epithelial apoptosis in the lung via p53 [76–78]. PPP1R13B may also promote apoptosis in a p53-independent manner by inhibiting autophagy in response to upregulation by EGR-1 (early growth response protein 1) [79]. EGR-1 mediates stress-induced proinflammatory responses in the airway epithelium and contributes to the pathogenesis of COPD [80–85]. Within the lung, *PPP1R13B* is indeed predominantly expressed in epithelial cells, particularly in alveolar type 2 cells, and less so in immune cells and fibroblasts [86,87]. However, Cheng and colleagues studied PPP1R13B function in lung fibroblasts and found that it was upregulated following SiO₂ exposure, where it promoted fibroblast proliferation and migration through endoplasmic reticulum stress and autophagy pathways [88]. Overall, these studies suggest that *PPP1R13B* plays a key role in maintaining tissue homeostasis by regulating apoptosis and autophagy in response to environmental stimuli [74,89,90]. The specific function(s) of this gene in the airway epithelium and its potential impact on the development of airway obstruction remain to be elucidated. *PPP1R13B* expression in airway epithelial cells at age 11 was not associated with lung function or urine cotinine levels in the URECA children, but the cofactors

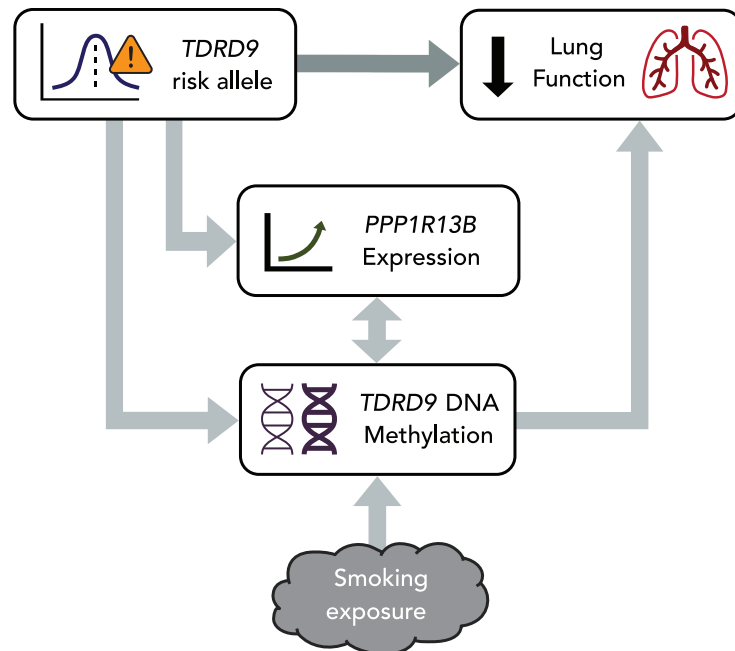


Fig 9. Summary of study associations. The *TDRD9* locus was significantly associated with FEV₁ (% predicted) in the APIC and URECA cohorts. This association was partially mediated by DNA methylation at the cg03306306 CpG site in *TDRD9* in NECs, which was also significantly associated with environmental tobacco smoke exposure. The *TDRD9* risk allele and DNA methylation were both significantly associated with *PPP1R13B* gene expression, but *PPP1R13B* gene expression was not significantly correlated with FEV₁ itself. Unidirectional arrows represent inferred causality.

<https://doi.org/10.1371/journal.pgen.1010594.g009>

of this gene [79,91] have been found previously to be upregulated in smokers with COPD [81,92]. Given its association with lung function alleles in our study, its expression in the airway epithelium, and its purported functions in autophagy and apoptosis pathways, additional study of *PPP1R13B* in lung and airway development is warranted, particularly in the context of adverse environmental stimuli, many of which are enriched in low-income urban environments.

In NECs, *PPP1R13B* gene expression was significantly associated with DNA methylation levels at the cg03306306 CpG site in *TDRD9*. Methylation at the *TDRD9* locus was previously reported to correlate with specific environmental exposures [67,68,93] and with *TDRD9* expression in blood [67,94]. *TDRD9* is lowly expressed in the lung but is detected in alveolar macrophages and in monocytes [86,87]. Interestingly, the gene was among the most differentially expressed genes in alveolar macrophages in smokers relative to non-smokers [95], and its knockdown in *TDRD9*-expressing lung carcinomas resulted in increased apoptosis [96]. Its expression was not correlated with the rs10220464 genotype in URECA NECs or PBMCs, but rs10220464 is an eQTL for *TDRD9* expression in whole blood in GTEx data [97], with the minor allele associated with lower *TDRD9* expression. Although evidence from this study points to *PPP1R13B* in the airway epithelium, we can't exclude the possibility that *TDRD9* or other genes could contribute to the locus' influence on lung function via other tissues.

The FEV₁ association signal at the *TDRD9* locus included many variants in high LD across a 200 kb region that could be independently contributing to function. Some of the variants lie in different long-range enhancers [59]. It is also possible that one or more correlated variants were not included because they failed quality control standards. In addition, due to the limited sample size of the WGS cohort, we excluded rare variants (MAF < 0.01) from consideration,

which could contribute to the signal at this locus. Additional functional studies are needed to identify the causal variant(s) and full mechanism of action.

The correlations of rs10220464, FEV₁, and smoking exposure with cg03306306 methylation in NECs were absent in PBMCs. Although global DNA methylation patterns between tissues are highly correlated [98], tissue-specific differentially methylated regions are more likely to be functional, particularly if they are positively correlated with gene expression [99]. The *TDRD9* locus has not been identified in epigenome-wide association studies of lung function [44,100–104], but these measured DNA methylation from blood, which may be an insufficient proxy for methylation in the lungs [105]. Indeed, previous studies have found that DNA methylation profiles in NECs are significantly more predictive of pediatric asthma than those in PBMCs [106,107]. Furthermore, epigenetic biomarkers can change with age. For example, epigenetic markers for lung function in adults do not replicate in children [101].

We tested for interactions between smoking exposure and rs10220464 genotype effects on cg03306306 and on FEV₁ and between smoking exposure and cg03306306 methylation effects on FEV₁. We did not detect any significant interactions, but our analyses in that regard could have been underpowered given our observed effects and sample sizes [36]. Furthermore, because this study was limited to children living in low-income urban neighborhoods, environmental risk factors are likely to be more prevalent than in the general population [55–57]. Additionally, such exposures are not necessarily ubiquitous across all the different neighborhoods and communities represented in this sample, and although environmental tobacco smoke exposure was examined and the socioeconomic range represented in this study is relatively narrow, there could be relevant environmental factors that were not considered.

To infer causality, Mendelian randomization and mediation analyses rely on assumptions that are often difficult to empirically verify. For the Mendelian randomization analysis, we identified instrumental variants associated with the intermediate cg03306306 that were not independently associated with the outcome, FEV₁. However, because these variants were selected from the same dataset that the outcome testing was performed in, they were susceptible to bias from winner's curse [108]. To mitigate the potential impact from this effect and from weak instruments, we performed a secondary analysis in which we combined the instrumental variants into a single, unweighted score. For the mediation analysis, unmeasured confounding can invalidate direct and indirect effect estimates [109]. To protect against such bias, we systematically tested for confounding associations with additional environmental measures available in APIC and URECA (Materials and methods). Nonetheless, there may still exist unknown confounding factors that were not measured. Ultimately the results of the Mendelian randomization and mediation analyses indicate that methylation at cg03306306 in NECs mediated the rs10220464 genotype effect on FEV₁, but there was residual correlation between rs10220464 and FEV₁, signifying that the genotype effect was only partially mediated by cg03306306.

Another limitation of our study was the relatively small size for a GWAS. This likely contributed to the lack of statistically significant replication for previously identified lung function loci [23], considering that the observed effects were correlated with results of prior GWAS. However, the APIC and URECA cohorts represent understudied, high-risk, pediatric populations that likely harbor distinct genetic and environmental risk factors compared to older, primarily European ancestry cohorts included in previous GWAS of lung function [14–20,23]. The findings of this study have yet to be replicated in an independent cohort, and should therefore be considered preliminary; however, it is possible that these associations would differ in populations with dissimilar ancestry, age, exposures, and/or asthma risk.

There are additional caveats to consider when interpreting our findings. First, this study integrated data from two cohorts with different recruitment criteria, asthma definitions, and

ancestral compositions. Furthermore, most of the analyses beyond the GWAS were limited to subsets of the URECA participants. However, we did not observe significant genetic effect heterogeneity for rs10220464 by study, asthma status, or ancestry. To control for potential population stratification, we used the first ten PCs of ancestry to adjust lung function values and then included the ancestry PCs as fixed effects in the GWAS models (Materials and methods). The linear mixed models also included a genetic relatedness matrix as a random effect to account for residual population structure. Because children with asthma have lower lung function overall (Table 1) and their lung function may be more affected by environmental exposures [110–112], we adjusted for asthma status in the GWAS, as in previous GWAS [113–116]. The likelihood of discovering lung function variants with consistent effects in asthmatics and non-asthmatics was thereby increased, although genetic determinants of lung function may differ by asthma status [117]. Furthermore, adjusting for disease status could potentially introduce collider bias [118]. The significant genotype effect at the *TDRD9* locus, however, remained the only genome-wide-significant association when asthma was excluded as a covariate, and adjustment for asthma did not substantively alter the mediation results. Second, some of the analyses used data collected at different timepoints. For example, most of the urine cotinine and spirometry measures were collected at age 10, but the samples used for the NEC DNA methylation and RNA-seq analyses were collected at age 11. Because DNA methylation and gene expression can change over time [40,119–121], their values at age 11 may not be fully representative of exposures at age 10. Finally, the promoter-capture Hi-C data were from lower airway (bronchial) epithelial cells, whereas the DNA methylation and RNA-seq data were generated from upper airway (nasal) epithelial cells. Although there are transcriptomic differences between epithelial cells from each compartment, their respective profiles are highly correlated [122–126], and the use of NECs as a proxy for the lower airway epithelium has been validated for both gene expression and epigenetic studies [124–127].

Our study identified a novel avenue through which genetic risk and environmental exposures could affect the airways of children raised in low-income urban neighborhoods. Further research into this pathway may yield mechanistic insights into the early development of impaired lung function, perhaps leading to interventions that can help reduce the high incidence and morbidity of chronic respiratory diseases in socioeconomically disadvantaged children.

Materials and methods

Ethics statement

The institutional review boards (IRBs) from all participating sites of the URECA (ClinicalTrials.gov Identifier: [NCT00114881](https://doi.org/10.1186/11745-014-0881)) and APIC (ClinicalTrials.gov Identifier: [NCT01383941](https://doi.org/10.1186/11745-014-08941)) studies gave initial ethical approval for this work. These include IRBs from the following institutions: National Jewish Health, Denver, CO (APIC); Children's National Medical Center, Washington, DC (APIC); Children's Memorial Hospital, Chicago, IL (APIC); Johns Hopkins University, Baltimore, MD (APIC & URECA); Boston University School of Medicine, Boston, MA (APIC); Henry Ford Health Center, Detroit, MI (APIC); Columbia University Medical Center, New York, NY (APIC & URECA); Cincinnati Children's Hospital, Cincinnati, OH (APIC); University of Texas Southwestern Medical School, Dallas, TX (APIC); Boston Medical Center, Boston, MA (URECA); Saint Louis Children's Hospital, Saint Louis, MO (URECA). In 2014, ethical oversight for these studies transitioned to a single, central IRB managed by WGC IRB (formerly Western IRB), whereupon WGC IRB gave ethical approval for this work [128]. Written informed consent was obtained from legal guardians of all participating children, who also assented.

Study population and phenotypes

We analyzed samples and phenotypes from two National Institutes of Allergy and Infectious Diseases (NIAID)-funded asthma studies conducted by the Inner-City Asthma Consortium (ICAC) [129]: the Asthma Phenotypes in the Inner City (APIC) study [55,56] and the Urban Environment and Childhood Asthma (URECA) birth cohort study [57]. The APIC study was a 1-year, prospective, epidemiological investigation of children and adolescents with asthma (ages 6–17) living in low-income areas ($\geq 20\%$ of residents below poverty level) in nine U.S. cities (Baltimore, MD; Boston, MA; Chicago, IL; Cincinnati, OH; Dallas, TX; Denver, CO; Detroit, MI; New York, NY; Washington, DC). The APIC participants were required to have a diagnosis of asthma by a physician and to have had at least two episodes requiring bronchodilator administration within the past year [55]. The URECA study enrolled pregnant women living in low-income areas of four U.S. cities (Baltimore, MD; Boston, MA; New York, NY; St. Louis, MO) who reported that either or both parents of the index pregnancy had a history of asthma or allergic diseases [57]. This prospective, longitudinal study followed each child through adolescence, periodically collecting samples and clinical and environmental exposure data.

Lung function was assessed using spirometry. Lung function measures used in this study for APIC participants were taken at the study entry visit (V0). For URECA, measurements from age 10 were used when available; otherwise, the most recent measurement after age 5 was used (S6 Table). Asthma status was assigned according to study-specific criteria. For APIC, asthma was defined by a doctor's diagnosis of asthma and short-acting beta-agonist use in the year prior [55]. For URECA, asthma status was determined either by doctor diagnosis, lung function reversibility, or symptom recurrence [130]. The 2012 Global Lung Initiative reference equations [131] were applied to generate percent predicted estimates for FEV₁ and Z-scores for FEV₁/FVC ratio. Urine cotinine levels were measured using NicAlert immunochromatographic assays, which report results on a scale of 0–6 according to different cotinine concentration ranges [132]. For URECA, urine cotinine results were available at age 10 for most participants (n = 391); otherwise, assays from age 8 (n = 29) or age 7 (n = 2) were used. This study utilized DNA methylation and RNA-seq data generated for other URECA studies; therefore, the number of samples included in each analysis varied and was limited by data availability (S7 Table, S12 Fig).

Whole-genome sequencing and data processing

DNA was extracted from peripheral blood (APIC, URECA) or cord blood (URECA) and quantified using an Invitrogen Qubit 3 Fluorometer. DNA quality was assessed using the Thermo Scientific NanoDrop One spectrophotometer and confirmed using an Agilent TapeStation system. DNA was processed in batches of 60 using the Illumina Nextera DNA Flex library prep kit with unique dual adaptors. Each set of 60 libraries was sequenced over two NovaSeq S4 flowcells. Whole-genome sequencing was performed by the University of Chicago Genomics Facility using the Illumina NovaSeq6000, which generated 150 bp paired-end reads. Sequencing data processing followed the Broad Institute's Genome Analysis Toolkit (GATK) best practices for germline short variant discovery, as implemented in the harmonized pipeline used by the New York Genome Center for TOPMed [133,134]. Reads were aligned to the GRCh38 human reference genome (including alternate loci and decoy contigs) using BWA-MEM (Burrows-Wheeler Aligner; v0.7.17). Aligned reads further underwent duplicate removal (Picard MarkDuplicates; v2.8.1) and base quality score recalibration (GATK BaseRecalibrator; v3.8) against known sites (dbSNP138, known InDels, and Mills and 1KG gold standard InDels) provided in the GATK resource bundle. Read alignment metrics were

calculated using Picard CollectWgsMetrics (v2.8.1) for all aligned reads and for aligned reads with base quality and mapping quality ≥ 20 . DNA contamination levels were estimated using VerifyBamID2 (v1.0.6) [135]. Samples with estimated DNA contamination >0.05 were removed from consideration. Samples with poor coverage ($<50\%$ of the genome with $\geq 20\times$ depth) were also removed from further consideration. To identify potential sample swaps, WGS samples were validated using independent genotyping arrays.

QC array for sample validation

To identify potential WGS sample swaps, we independently genotyped the APIC and URECA participants using the Illumina QC Array-24 BeadChip. SNPs were tested for Hardy-Weinberg Equilibrium (HWE) within each self-identified ancestry group using the chi-square test and removed if they deviated from HWE (Bonferroni-adjusted $p < 0.05$) within at least one ancestry. SNPs with call rates <0.98 were also removed. Samples with total variant call rates <0.95 were not used. Array data with incorrect or indeterminate sex according to X-chromosome heterozygosity rates (Plink v1.90) were also not used [136]. For fourteen of the sequenced URECA samples, we used results from the Illumina Infinium CoreExome+Custom array for sample validation, which were generated and controlled for quality as described by McKennan and colleagues [137]. WGS and array genotypes were tested for concordance using VerifyBamID (v1.1.3) [138]. WGS samples that were not validated with array data were not included in genetic analyses ($n = 2$).

Variant calling and quality control

Variant calls were generated using GATK HaplotypeCaller (v4.1.3.0), accounting for contamination estimates, for single nucleotide variants and short insertions, deletions, and substitutions. Sample genotypes were joined using GATK GenomicsDBImport and GenotypeGVCFs over the genomic intervals defined in the GATK WGS calling region interval list provided in the GATK resource bundle. Genotypes with read depth (DP) <10 or quality scores (GQ) <20 were set as missing. Sites with ≥ 0.1 missingness were then removed from consideration. Variants with minor allele frequencies >0.05 were tested for accordance with HWE, accounting for population structure [139]. Sites with common variants that deviated from structural HWE ($P < 1 \times 10^{-6}$) were removed from consideration. Sites with quality by depth ratios (QD) <4 or >34 were also removed, as we observed declines in variant transition/transversion (TS/TV) ratios beyond these bounds (S13 Fig). Variant site quality was further evaluated using machine-learning-based Variant Quality Score Recalibration (VQSR). First, SNPs were modeled using GATK VariantRecalibrator (v4.1.3.0) with Hapmap 3 and with Omni 2.5M SNP chip array as truth resources, 1000G as a training resource, and dbSNP138 as a known sites resource. InDels were likewise trained with the Mills and 1KG gold standard InDels dataset as a truth resource and dbSNP138 as a known sites resource. SNPs and InDels with resultant predicted true positive probabilities below 0.997 and 0.990, respectively, were removed from consideration. Variant call accuracy was assessed by comparing call concordance between three replicate sequencing samples using VCFtools (v0.1.14) vcf-compare [140]. Variant call file manipulation was conducted using BCFtools (v1.10.2) [141].

Ancestry estimation

Ancestry principal components (PCs) were calculated on the intersect of high quality single-nucleotide variants (SNVs) genotyped in the WGS data and several reference panels from the 1000 Genomes Project (1KG; $n = 156$) [142] and the Human Genome Diversity Project (HGDP; $n = 52$) [143]. Native American reference samples consisted of 52 samples from the

HGDP with <5% non-native ancestry, according to an analysis of roughly 2 million markers using the program ADMIXTURE (v1.3.0) [144]. These samples were filtered for site quality (missingness 5%; ExcHet<60; VQSLOD \geq 8.3929), genotype quality (GQ \geq 20) and depth (DP \geq 10), MAF >0.02, and HWE ($p>0.001$) [143]. European, West African, and East Asian reference samples were randomly selected from CEU (n = 52), YRI (n = 52), JPT (n = 26), and CHB (n = 26) samples in the phase 3 1KG reference panel [142]. The combined genotypes were pruned for linkage disequilibrium (LD) ≤ 0.1 within 1Mb intervals. Ancestry PCs were calculated, accounting for subject relatedness, using PC-Air [145] and PC-Relate [146]. Initial kinship estimates were produced using KING [147]. Kinship and PCs were iteratively estimated using PC-Relate and PC-Air, respectively, until estimates for the top 5 PCs stabilized (n = 3). Reference population admixture estimates were estimated for each WGS sample with ADMIXTURE (v1.3.0), using the 1KG and HGDP reference samples for supervised analysis [144]. Because sample relatedness can lead to biased admixture estimates [145,148], admixture was estimated for each WGS sample separately.

Quantitative trait association testing

Quantitative traits were adjusted for covariates and normalized using a two-stage approach [149,150]. First, each trait was regressed on age, sex, asthma status, and the first 10 PCs of ancestry. The residuals were then rank-normalized using an inverse normal transformation. In the second stage, the normalized residuals were considered outcome variables in the GWAS, adjusting for the same covariates as in the first stage. Genome-wide association testing was performed for all high-quality common variant calls (MAF \geq 0.01) using a linear mixed model, as implemented in GEMMA [58], with subject relatedness included as a random effect. Individuals who were not evaluated for asthma at ages 7 or 10 (n = 127) were excluded from trait association testing. The threshold we applied for genome-wide significance was $P\leq 2.5\times 10^{-8}$, based on a 5×10^{-8} GWAS threshold and further accounting for two tests. To identify potential collider bias introduced by adjusting for asthma status, we repeated the GWAS without accounting for asthma status in either covariate-adjustment stage.

Fine-mapping analysis was conducted using SuSiE (SusieR R package v0.12.27) [151]. SuSiE applies a form of Bayesian variable selection in regression using iterative Bayesian step-wise selection to identify “credible sets” of variables. Each credible set has a 95% probability of containing at least one causal effect SNP. Prior to running SuSiE, we regressed asthma, age, sex, and ancestry PCs 1–10 from the genotype matrix and outcome vector (the normalized FEV₁ residuals).

To explore whether there was lead-SNP effect heterogeneity by ancestry, study, or asthma status, we performed additional single-SNP quantitative trait association tests within several different sub-cohorts and introduced interaction effects into our models. For ancestry, we performed separate association tests in each of the non-Hispanic Black, Hispanic, and white populations, according to self-identified race/ethnicity. We then tested for genotype-by-ancestry interaction effects across APIC and URECA by using admixture proportions as covariates in our models, in lieu of ancestry PCs, and including an interaction term with the lead SNP for each continental ancestry group in turn. We tested these interaction effects using the—gxe argument in GEMMA in four separate models (one for each ancestry). To determine whether there was effect heterogeneity by study (APIC vs. URECA), we performed separate association tests in each study and also tested the association across APIC and URECA with the addition of a study covariate and a genotype-by-study interaction term. For asthma status, we performed separate association tests in the asthmatics and non-asthmatics and tested a genotype interaction term with asthma status.

DNA methylation analysis

DNA from NECs was collected at age 11 from 287 URECA participants and assessed for genome-wide methylation patterns using the Illumina Infinium Human Methylation EPIC Beadchip. DNA methylation levels from PBMCs at age 7 in URECA were collected and processed as previously described [66]. MeQTL analysis was performed using Matrix eQTL [152]. NEC DNA methylation levels were adjusted globally for sex, array, plate, collection site, DNA concentration, percent ciliated epithelial cells, percent squamous cells, and ancestry PCs 1–3. Principal components analysis was then performed on the residual methylation levels, and the first three PCs were included as covariates in the meQTL association tests. Additional methylation PCs were not included in association tests, as they were significantly correlated with asthma phenotypes. Associations with FDR-adjusted $P < 0.05$ were considered significant. MeQTL analysis with the PBMC data included sex, collection site, plate, ancestry PCs 1–3, and eight latent factors [153] (protecting for FEV_1 at age 7) as covariates.

To test CpG site methylation associations with lung function in NECs, we performed linear regressions on the most recent FEV_1 measures, with age, sex, ancestry PCs 1–3, and methylation PCs 1–3 as covariates. For the PBMC analysis, we set FEV_1 at age 7 as the dependent variable, with sex, collection site, plate, ancestry PCs 1–3, and latent factors included as covariates.

For association testing with smoking exposures, we ran linear regressions for DNA methylation and lung function in NECs and PBMCs, as described above, with the addition of cotinine concentrations as a predictor. We further tested for smoking-by-genotype interaction effects on DNA methylation and lung function using these models by adding an interaction term (cotinine concentration: rs10220464 genotype). Proportions of explained variance were calculated by squaring partial correlation coefficients of regression model predictors [154]. One sample from one sibling pair was removed from all methylation analyses to prevent confounding due to relatedness.

Mendelian randomization and mediation analysis

To assess the causal effects of DNA methylation on lung function, we performed one-sample Mendelian randomization analysis. We applied a 2SLS regression to URECA samples with WGS and DNA methylation data ($n = 285$) using ivreg [155]. DNA methylation levels in NECs at the cg03306306 CpG site were first adjusted for methylation PCs 1–3 and used as the endogenous, exposure variable. The adjusted and normalized FEV_1 values from the GWAS were set as the dependent outcome variable. Urine cotinine levels were included as an exogenous covariate (included in both stages). The instrumental variables were chosen from a set of candidate SNPs that were at least nominally associated with cg03306306 methylation with $p < 0.15$. Clustering of pairwise linkage disequilibrium values between these SNPs revealed six distinct haplotypes (S14 Fig). To ensure instrument exogeneity, each candidate SNP was tested for association with FEV_1 after conditioning on cg03306306 methylation and urine cotinine, and SNPs associated with $p < 0.05$ were removed from consideration. Of the remaining candidate SNPs, one was chosen from each haplotype, resulting in an instrument composed of 4 SNPs (rs11160777, rs137961671, rs7143936, rs11160776). Instrument relevance was validated using the F test, endogeneity using the Wu-Hausman test, and instrument exogeneity using the Sargon test. We tested two 2SLS models: one where the instrumental variables were included as individual predictors, and another featuring an unweighted allele score of the four instrumental variants to reduce potential bias from weak instruments and/or winner's curse [156,157].

Mediation analysis was conducted with ROBMED [158]. The adjusted and normalized FEV_1 residuals were set as the dependent variable, adjusted cg03306306 methylation as the mediator,

and rs10220464 as the independent variable. Age at FEV₁ measurement, sex, asthma status, ancestry PCs 1–3, and urine cotinine levels were included as covariates. We also performed a secondary mediation analysis without adjusting for asthma status. To identify additional, potential confounders that could invalidate our mediation model, we systematically tested for associations with 2 socioeconomic variables and 11 environmental exposures available in APIC and URECA (S8 Table, S15 Fig). For each environmental exposure, we tested whether the variable was associated with the mediator (cg03306306) and whether the variable was associated with the outcome (FEV₁) conditional on the mediator. To ensure no exposure-mediator interactions, we repeated the cg03306306 association test with FEV₁ with rs10220464 included as a predictor with a rs10220464: cg03306306 interaction term. The indirect effect of rs10220464 on FEV₁ via cg03306306 methylation was estimated using 100,000 bootstrap resamples.

Gene expression analysis

We analyzed gene expression in NECs and PBMCs from the URECA birth cohort using RNA-seq. The NEC data were derived from 323 children (155 females, 168 males) at age 11 years at the time of sample collection, and the PBMC data were derived from 130 (53 females, 77 males) PBMC children aged 2 years at the time of collection. Sequencing reads were mapped and quantified using STAR (v2.6.1) [159] and samples underwent trimmed means of M-value (TMM) normalization and voom transformation [160]. Genes with <1 count per million mapped reads (CPM) were removed from analysis. For eQTL association testing in NECs we corrected for sex, the first three ancestry PCs, collection site, epithelial cell proportion, sequencing batch, and 14 latent factors [153] using limma [161]. In PBMCs, we corrected for sex, the first three ancestry PCs, collection site, and 19 latent factors.

Chromatin interaction analysis

Chromatin interactions were assessed using promoter capture Hi-C [162,163] in ex vivo human BECs from 8 adult lung donors, including 4 with asthma. The data were processed and analyzed as previously described [72,164]. Chromosomal interactions were evaluated using the CHiCAGO algorithm [165]. Interactions with CHiCAGO scores ≥ 5 were considered significant [165]. Genetic variants within 1 kb of a given interacting fragment were considered part of the chromatin loop. Genes that were not expressed in NECs were not included in the analysis.

Supporting information

S1 Fig. Whole-genome sequencing depth and coverage. A) Histogram of 1,035 whole-genome sequencing (WGS) samples from APIC and URECA by mean depth of coverage. B) Histogram of WGS samples based on proportion of genome covered at 20x, 25x, and 30x depth. APIC, Asthma Phenotypes in the Inner City study; URECA, Urban Environment and Childhood Asthma study. (PDF)

S2 Fig. Distribution of lung function measures by study. A) Distribution of FEV₁ (% predicted) in APIC and URECA. B) Distribution of FEV₁/FVC in APIC and URECA. APIC, Asthma Phenotypes in the Inner City study; URECA, Urban Environment and Childhood Asthma study. FEV₁, forced expiratory volume in one second; FVC, forced vital capacity. (PDF)

S3 Fig. P-value distributions of GWAS results. Quantile-quantile plots of the GWAS results with corresponding genomic control factors (λ) are shown for A) FEV₁ (% predicted)

and B) FEV₁/FVC. FEV₁, forced expiratory volume in one second; FVC, forced vital capacity. (PDF)

S4 Fig. Fine-mapping results for FEV₁ (% predicted) at the *TDRD9* locus. The X-axis shows the chromosome position on chromosome 14. The Y-axis is the posterior inclusion probability (PIP). Variants highlighted in red represent a credible set, in which there is a 95% probability that at least one of the variants is causal. FEV₁, forced expiratory volume in one second. (PDF)

S5 Fig. Genome-wide association results without adjustment for asthma. GWAS Manhattan plots for A) FEV₁ and B) FEV₁/FVC ratio, without adjustment for asthma status. The horizontal red line indicates genome-wide significance ($p \leq 2.5 \times 10^{-8}$). The dotted horizontal blue line indicates $p = 1 \times 10^{-5}$. Variants colored in grey are the GWAS results with asthma adjustment. FEV₁, forced expiratory volume in one second; FEV₁/FVC, ratio of FEV₁ to forced vital capacity. (PDF)

S6 Fig. Replication of FEV₁ GWAS SNPs. Association statistics for previously identified FEV₁ GWAS SNPs [23]. 64 out of 70 previously identified SNPs were genotyped in APIC & URECA. GWAS, genome-wide association study; SNP, single nucleotide polymorphism; APIC, Asthma Phenotypes in the Inner City study; URECA, Urban Environment and Childhood Asthma study. FEV₁, forced expiratory volume in one second. (PDF)

S7 Fig. Replication of FEV₁/FVC GWAS SNPs. Association statistics for previously identified FEV₁/FVC GWAS SNPs [23]. 112 out of 117 previously identified SNPs were genotyped in APIC & URECA. GWAS, genome-wide association study; SNP, single nucleotide polymorphism; APIC, Asthma Phenotypes in the Inner City study; URECA, Urban Environment and Childhood Asthma study. FEV₁, forced expiratory volume in one second; FVC, forced vital capacity. (PDF)

S8 Fig. NicAlert Results by Study. Distribution of urine cotinine levels, as measured using NicAlert immunochromatographic assays, which report results on a scale of 0–6 according to the labeled concentration ranges. Proportions were calculated relative to the number of samples with available NicAlert results. APIC, Asthma Phenotypes in the Inner City study; URECA, Urban Environment and Childhood Asthma study. (PDF)

S9 Fig. DNA methylation at cg03306306 by smoking exposure. DNA methylation levels at cg03306306 are shown by rs10220464 genotype in URECA participants with low and high smoking exposures in (A) NECs at age 11 and (B) PBMCs at age 7. FEV₁ (% predicted) are also shown by cg03306306 DNA methylation levels in URECA participants with low and high smoking exposures in (C) NECs at age 11 and (D) PBMCs at age 7. NECs, nasal epithelial cells; PBMCs, peripheral blood mononuclear cells; FEV₁, forced expiratory volume in one second; URECA, Urban Environment and Childhood Asthma study. (PDF)

S10 Fig. Genotype associations with FEV₁ by smoking exposure. FEV₁ (% predicted) are shown by rs10220464 genotype in APIC & URECA participants with low and high smoking exposures according to urine cotinine levels. FEV₁, forced expiratory volume in one second; APIC, Asthma Phenotypes in the Inner City study; URECA, Urban Environment and

Childhood Asthma study.
(PDF)

S11 Fig. *PPP1R13B* expression in NECs vs. smoking exposure, FEV₁. *PPP1R13B* expression in NECs at age 11 was not associated with smoking exposure at age 10 (A) nor with FEV₁ (% predicted) at age 10 (B) in URECA. NECs, nasal epithelial cells; FEV₁, forced expiratory volume in one second; URECA, Urban Environment and Childhood Asthma.
(PDF)

S12 Fig. Data availability across APIC and URECA. Data availability for measures used in this study are shown for all sequenced samples. Each row represents a pattern of available and missing data, with green squares indicating available data and grey squares indicating missing data. Total counts of available data points for each variable are listed across the top of the figure. Total counts for each data availability pattern are listed along the right.
(PDF)

S13 Fig. Transitions/transversions vs. quality/depth in WGS variant calls. The transition/transversion ratio (TS/TV) is plotted against the variant call quality/depth metric (QD) across all WGS SNP calls in APIC & URECA. Sites with QD less than 4 or greater than 34 were removed from consideration in this study. SNPs, single nucleotide polymorphisms; WGS, whole-genome sequencing; APIC, Asthma Phenotypes in the Inner City study; URECA, Urban Environment and Childhood Asthma study.
(PDF)

S14 Fig. Intercorrelation of Mendelian randomization candidate instrument SNPs in URECA. Instrumental variables were chosen from a set of candidate SNPs that were at least nominally associated with cg03306306 methylation with $p < 0.15$. The correlation values between these SNPs are shown, clustered using Ward's method. The four SNPs used for the instrument are highlighted. URECA, Urban Environment and Childhood Asthma.
(PDF)

S15 Fig. Intercorrelation of phenotypes and environmental variables in APIC & URECA. The correlations are shown between FEV₁ (% predicted), smoking exposure (NicAlert), the primary the lead FEV₁ SNP rs10220464, DNA methylation at cg03306306, 11 environmental exposures, and 2 socioeconomic indicators, clustered using Ward's method. APIC, Asthma Phenotypes in the Inner City study; exp., exposure; URECA, Urban Environment and Childhood Asthma.
(PDF)

S1 Table. Post-QC sequencing call concordance between replicates. Variant call concordance between three pairs of replicate samples, by variant type and cohort allele frequency. SNPs, single nucleotide polymorphisms; MAF, minor allele frequency; InDels, insertions and deletions.
(PDF)

S2 Table. FEV₁-associated variants in chr14q32.33. All variants in chr14q32.33 associated with FEV₁ (% predicted) with $p < 1 \times 10^{-5}$ ($n = 82$) in GWAS of 896 participants from APIC & URECA. N, number of genotyped individuals. MAF, minor allele frequency; 95% CI, 95% confidence interval; SE, standard error; P, P-value (Wald); FEV₁, forced expiratory volume in one second; APIC, Asthma Phenotypes in the Inner City study; URECA, Urban Environment and Childhood Asthma study.
(PDF)

S3 Table. MeQTL analysis results and associations with FEV₁. All CpG sites where DNA methylation levels in NECs at age 11 in URECA were associated with rs10220464 at FDR<0.05 are shown with their corresponding associations with FEV₁. The FDR-adjusted P-values (FDR Q) correspond to a 5% false-discovery rate. FDR, false discovery rate; 95% CI, 95% confidence interval; FEV₁, forced expiratory volume in one second; URECA, Urban Environment and Childhood Asthma study.

(PDF)

S4 Table. rs10220464 eQTL analysis results. Results of eQTL analyses in NECs and PBMCs with rs10220464 for all genes within 1 Mb in URECA. Gene expression was measured in counts per million mapped reads. The FDR-adjusted P-values (FDR Q) correspond to a 5% false-discovery rate. FDR, false discovery rate; 95% CI, 95% confidence interval; NECs, nasal epithelial cells; PBMCs, peripheral blood mononuclear cells; URECA, Urban Environment and Childhood Asthma study.

(PDF)

S5 Table. Chromatin interactions with FEV₁-associated SNPs. Bait and target fragments refer to mapped Hi-C restriction fragments on chr14 (hg38) for gene promoters and putative enhancers, respectively. FEV₁ SNPs refer to number of FEV₁-associated variants ($p < 1 \times 10^{-5}$) within 1kb of target fragment. SNPs, single nucleotide polymorphisms; FEV₁, forced expiratory volume in one second.

(PDF)

S6 Table. Age at used lung function measure in URECA. URECA, Urban Environment and Childhood Asthma study; FEV₁, forced expiratory volume in one second; FVC, forced vital capacity.

(PDF)

S7 Table. Study samples. APIC, Asthma Phenotypes in the Inner City study; URECA, Urban Environment and Childhood Asthma study; WGS, whole-genome sequencing; NECs, nasal epithelial cells; PBMCs, peripheral blood mononuclear cells.

(PDF)

S8 Table. Additional phenotypic, socioeconomic, and environmental data. Additional variables examined for potential confounding in mediation analyses for APIC & URECA. APIC, Asthma Phenotypes in the Inner City study; URECA, Urban Environment and Childhood Asthma study.

(PDF)

Acknowledgments

We are grateful to all participants and their families who took part in these studies. We would like to extend special thanks to Pieter Faber and the University of Chicago Genomics Facility, as well as to Petra LeBeau and Rebecca Z. Krouse, formerly of Rho Inc., for their respective contributions.

Author Contributions

Conceptualization: Matthew Dapas, William W. Busse, James E. Gern, Daniel J. Jackson, Carole Ober.

Data curation: Matthew Dapas, Emma E. Thompson, William Wentworth-Sheilds, Cynthia M. Visness, Agustin Calatroni.

Formal analysis: Matthew Dapas, Emma E. Thompson, Selene Clay, Agustin Calatroni, Joanne E. Sordillo, Matthew C. Altman.

Funding acquisition: Matthew Dapas, William W. Busse, James E. Gern, Daniel J. Jackson, Carole Ober.

Investigation: Matthew Dapas, Robert A. Wood, Melanie Makhija, Gurjit K. Khurana Hershey, Michael G. Sherenian, Rebecca S. Gruchalla, Michelle A. Gill, Andrew H. Liu, Haejin Kim, Meyer Kattan, Deepa Rastogi, George T. O'Connor.

Methodology: Matthew Dapas, Dan Nicolae.

Project administration: Matthew Dapas, William Wentworth-Sheilds, Cynthia M. Visness, Leonard B. Bacharier, William W. Busse, Patrice M. Becker, George T. O'Connor, James E. Gern, Daniel J. Jackson, Carole Ober.

Resources: Carole Ober.

Software: Matthew Dapas.

Supervision: Cynthia M. Visness, Leonard B. Bacharier, William W. Busse, Patrice M. Becker, Dan Nicolae, George T. O'Connor, James E. Gern, Daniel J. Jackson, Carole Ober.

Validation: Matthew Dapas, Joanne E. Sordillo, Diane R. Gold.

Visualization: Matthew Dapas.

Writing – original draft: Matthew Dapas.

Writing – review & editing: Matthew Dapas, George T. O'Connor, James E. Gern, Daniel J. Jackson, Carole Ober.

References

1. Hole DJ, Watt GC, Davey-Smith G, Hart CL, Gillis CR, Hawthorne VM. Impaired lung function and mortality risk in men and women: findings from the Renfrew and Paisley prospective population study. *BMJ*. 1996; 313(7059):711–5; discussion 5–6. <https://doi.org/10.1136/bmj.313.7059.711> PMID: 8819439
2. Schunemann HJ, Dorn J, Grant BJ, Winkelstein W Jr., Trevisan M. Pulmonary function is a long-term predictor of mortality in the general population: 29-year follow-up of the Buffalo Health Study. *Chest*. 2000; 118(3):656–64.
3. Mannino DM, Holguin F, Pavlin BI, Ferdinands JM. Risk factors for prevalence of and mortality related to restriction on spirometry: findings from the First National Health and Nutrition Examination Survey and follow-up. *Int J Tuberc Lung Dis*. 2005; 9(6):613–21. PMID: 15971387
4. Chinn S, Gislason T, Aspelund T, Gudnason V. Optimum expression of adult lung function based on all-cause mortality: results from the Reykjavik study. *Respir Med*. 2007; 101(3):601–9. <https://doi.org/10.1016/j.rmed.2006.06.009> PMID: 16889951
5. Miller MR, Pedersen OF, Lange P, Vestbo J. Improved survival prediction from lung function data in a large population sample. *Respir Med*. 2009; 103(3):442–8. <https://doi.org/10.1016/j.rmed.2008.09.016> PMID: 18993043
6. Agusti A, Noell G, Brugada J, Faner R. Lung function in early adulthood and health in later life: a trans-generational cohort analysis. *Lancet Respir Med*. 2017; 5(12):935–45. [https://doi.org/10.1016/S2213-2600\(17\)30434-4](https://doi.org/10.1016/S2213-2600(17)30434-4) PMID: 29150410
7. Stern DA, Morgan WJ, Wright AL, Guerra S, Martinez FD. Poor airway function in early infancy and lung function by age 22 years: a non-selective longitudinal cohort study. *Lancet*. 2007; 370(9589):758–64. [https://doi.org/10.1016/S0140-6736\(07\)61379-8](https://doi.org/10.1016/S0140-6736(07)61379-8) PMID: 17765525
8. Stocks J, Hislop A, Sonnappa S. Early lung development: lifelong effect on respiratory health and disease. *Lancet Respir Med*. 2013; 1(9):728–42. [https://doi.org/10.1016/S2213-2600\(13\)70118-8](https://doi.org/10.1016/S2213-2600(13)70118-8) PMID: 24429276

9. McGeachie MJ, Yates KP, Zhou X, Guo F, Sternberg AL, Van Natta ML, et al. Patterns of Growth and Decline in Lung Function in Persistent Childhood Asthma. *N Engl J Med*. 2016; 374(19):1842–52. <https://doi.org/10.1056/NEJMoa1513737> PMID: 27168434
10. Agusti A, Faner R. Lung function trajectories in health and disease. *Lancet Respir Med*. 2019; 7(4):358–64. [https://doi.org/10.1016/S2213-2600\(18\)30529-0](https://doi.org/10.1016/S2213-2600(18)30529-0) PMID: 30765254
11. Bisgaard H, Jensen SM, Bonnelykke K. Interaction between asthma and lung function growth in early life. *Am J Respir Crit Care Med*. 2012; 185(11):1183–9. <https://doi.org/10.1164/rccm.201110-1922OC> PMID: 22461370
12. Duijts L, Reiss IK, Brusselle G, de Jongste JC. Early origins of chronic obstructive lung diseases across the life course. *Eur J Epidemiol*. 2014; 29(12):871–85. <https://doi.org/10.1007/s10654-014-9981-5> PMID: 25537319
13. Klimentidis YC, Vazquez AI, de Los Campos G, Allison DB, Dransfield MT, Thannickal VJ. Heritability of pulmonary function estimated from pedigree and whole-genome markers. *Front Genet*. 2013; 4:174. <https://doi.org/10.3389/fgene.2013.00174> PMID: 24058366
14. Wilk JB, Chen TH, Gottlieb DJ, Walter RE, Nagle MW, Brandler BJ, et al. A genome-wide association study of pulmonary function measures in the Framingham Heart Study. *PLoS Genet*. 2009; 5(3):e1000429. <https://doi.org/10.1371/journal.pgen.1000429> PMID: 19300500
15. Repapi E, Sayers I, Wain LV, Burton PR, Johnson T, Obeidat M, et al. Genome-wide association study identifies five loci associated with lung function. *Nat Genet*. 2010; 42(1):36–44. <https://doi.org/10.1038/ng.501> PMID: 20010834
16. Hancock DB, Eijgelsheim M, Wilk JB, Gharib SA, Loehr LR, Marcicante KD, et al. Meta-analyses of genome-wide association studies identify multiple loci associated with pulmonary function. *Nat Genet*. 2010; 42(1):45–52. <https://doi.org/10.1038/ng.500> PMID: 20010835
17. Soler Artigas M, Loth DW, Wain LV, Gharib SA, Obeidat M, Tang W, et al. Genome-wide association and large-scale follow up identifies 16 new loci influencing lung function. *Nat Genet*. 2011; 43(11):1082–90. <https://doi.org/10.1038/ng.941> PMID: 21946350
18. Yao TC, Du G, Han L, Sun Y, Hu D, Yang JJ, et al. Genome-wide association study of lung function phenotypes in a founder population. *J Allergy Clin Immunol*. 2014; 133(1):248–55 e1-10. <https://doi.org/10.1016/j.jaci.2013.06.018> PMID: 23932459
19. Loth DW, Soler Artigas M, Gharib SA, Wain LV, Franceschini N, Koch B, et al. Genome-wide association analysis identifies six new loci associated with forced vital capacity. *Nat Genet*. 2014; 46(7):669–77. <https://doi.org/10.1038/ng.3011> PMID: 24929828
20. Wain LV, Shrine N, Artigas MS, Erzurumluoglu AM, Noyvert B, Bossini-Castillo L, et al. Genome-wide association analyses for lung function and chronic obstructive pulmonary disease identify new loci and potential druggable targets. *Nat Genet*. 2017; 49(3):416–25. <https://doi.org/10.1038/ng.3787> PMID: 28166213
21. Burkart KM, Sofer T, London SJ, Manichaikul A, Hartwig FP, Yan Q, et al. A Genome-Wide Association Study in Hispanics/Latinos Identifies Novel Signals for Lung Function. *The Hispanic Community Health Study/Study of Latinos*. *Am J Respir Crit Care Med*. 2018; 198(2):208–19. <https://doi.org/10.1164/rccm.201707-1493OC> PMID: 29394082
22. Wyss AB, Sofer T, Lee MK, Terzikhan N, Nguyen JN, Lahousse L, et al. Multiethnic meta-analysis identifies ancestry-specific and cross-ancestry loci for pulmonary function. *Nat Commun*. 2018; 9(1):2976. <https://doi.org/10.1038/s41467-018-05369-0> PMID: 30061609
23. Shrine N, Guyatt AL, Erzurumluoglu AM, Jackson VE, Hobbs BD, Melbourne CA, et al. New genetic signals for lung function highlight pathways and chronic obstructive pulmonary disease associations across multiple ancestries. *Nat Genet*. 2019; 51(3):481–93. <https://doi.org/10.1038/s41588-018-0321-7> PMID: 30804560
24. Akenroye AT, Brunetti T, Romero K, Daya M, Kanchan K, Shankar G, et al. Genome-wide association study of asthma, total IgE, and lung function in a cohort of Peruvian children. *J Allergy Clin Immunol*. 2021. <https://doi.org/10.1016/j.jaci.2021.02.035> PMID: 33713768
25. Zhu Z, Li J, Si J, Ma B, Shi H, Lv J, et al. A large-scale genome-wide association analysis of lung function in the Chinese population identifies novel loci and highlights shared genetic aetiology with obesity. *Eur Respir J*. 2021; 58(4). <https://doi.org/10.1183/13993003.00199-2021> PMID: 33766948
26. Obeidat M, Hao K, Bosse Y, Nickle DC, Nie Y, Postma DS, et al. Molecular mechanisms underlying variations in lung function: a systems genetics analysis. *Lancet Respir Med*. 2015; 3(10):782–95. [https://doi.org/10.1016/S2213-2600\(15\)00380-X](https://doi.org/10.1016/S2213-2600(15)00380-X) PMID: 26404118
27. Gharib SA, Loth DW, Soler Artigas M, Birkland TP, Wilk JB, Wain LV, et al. Integrative pathway genomics of lung function and airflow obstruction. *Hum Mol Genet*. 2015; 24(23):6836–48. <https://doi.org/10.1093/hmg/ddv378> PMID: 26395457

28. Portas L, Pereira M, Shaheen SO, Wyss AB, London SJ, Burney PGJ, et al. Lung Development Genes and Adult Lung Function. *Am J Respir Crit Care Med*. 2020; 202(6):853–65. <https://doi.org/10.1164/rccm.201912-2338OC> PMID: 32392078
29. Kheirallah AK, Miller S, Hall IP, Sayers I. Translating Lung Function Genome-Wide Association Study (GWAS) Findings: New Insights for Lung Biology. *Adv Genet*. 2016; 93:57–145. <https://doi.org/10.1016/bs.adgen.2015.12.002> PMID: 26915270
30. Aschard H, Tobin MD, Hancock DB, Skurnik D, Sood A, James A, et al. Evidence for large-scale gene-by-smoking interaction effects on pulmonary function. *Int J Epidemiol*. 2017; 46(3):894–904. <https://doi.org/10.1093/ije/dyw318> PMID: 28082375
31. Park B, An J, Kim W, Kang HY, Koh SB, Oh B, et al. Effect of 6p21 region on lung function is modified by smoking: a genome-wide interaction study. *Sci Rep*. 2020; 10(1):13075. <https://doi.org/10.1038/s41598-020-70092-0> PMID: 32753590
32. Kim W, Moll M, Qiao D, Hobbs BD, Shrine N, Sakornsakolpat P, et al. Smoking Interaction with a Polygenic Risk Score for Reduced Lung Function. *medRxiv*. 2021. <https://doi.org/10.1101/2021.03.26.21254415>
33. Melbourne CA, Erzurumluoglu AM, Shrine N, Chen J, Tobin MD, Hansell A, et al. Genome-wide gene-air pollution interaction analysis of lung function in 300,000 individuals. *medRxiv*. 2021. <https://doi.org/10.1016/j.envint.2021.107041> PMID: 34923368
34. Miller MD, Marty MA. Impact of environmental chemicals on lung development. *Environ Health Perspect*. 2010; 118(8):1155–64. <https://doi.org/10.1289/ehp.0901856> PMID: 20444669
35. Decrue F, Gorlanova O, Usemann J, Frey U. Lung functional development and asthma trajectories. *Semin Immunopathol*. 2020; 42(1):17–27. <https://doi.org/10.1007/s00281-020-00784-2> PMID: 31989229
36. He Z, Wu H, Zhang S, Lin Y, Li R, Xie L, et al. The association between secondhand smoke and childhood asthma: A systematic review and meta-analysis. *Pediatr Pulmonol*. 2020; 55(10):2518–31. <https://doi.org/10.1002/ppul.24961> PMID: 32667747
37. Thacher JD, Schultz ES, Hallberg J, Hellberg U, Kull I, Thunqvist P, et al. Tobacco smoke exposure in early life and adolescence in relation to lung function. *Eur Respir J*. 2018; 51(6).
38. Dratva J, Zemp E, Dharmage SC, Accordini S, Burdet L, Gislason T, et al. Early Life Origins of Lung Ageing: Early Life Exposures and Lung Function Decline in Adulthood in Two European Cohorts Aged 28–73 Years. *PLoS One*. 2016; 11(1):e0145127. <https://doi.org/10.1371/journal.pone.0145127> PMID: 26811913
39. Savran O, Ulrik CS. Early life insults as determinants of chronic obstructive pulmonary disease in adult life. *Int J Chron Obstruct Pulmon Dis*. 2018; 13:683–93. <https://doi.org/10.2147/COPD.S153555> PMID: 29520136
40. Zeilinger S, Kuhnel B, Klopp N, Baurecht H, Kleinschmidt A, Gieger C, et al. Tobacco smoking leads to extensive genome-wide changes in DNA methylation. *PLoS One*. 2013; 8(5):e63812. <https://doi.org/10.1371/journal.pone.0063812> PMID: 23691101
41. Rider CF, Carlsten C. Air pollution and DNA methylation: effects of exposure in humans. *Clin Epigenetics*. 2019; 11(1):131. <https://doi.org/10.1186/s13148-019-0713-2> PMID: 31481107
42. Jamieson E, Korologou-Linden R, Wootton RE, Guyatt AL, Battram T, Burrows K, et al. Smoking, DNA Methylation, and Lung Function: a Mendelian Randomization Analysis to Investigate Causal Pathways. *Am J Hum Genet*. 2020; 106(3):315–26. <https://doi.org/10.1016/j.ajhg.2020.01.015> PMID: 32084330
43. Kwak SY, Park CY, Shin MJ. Smoking May Affect Pulmonary Function through DNA Methylation: an Epigenome-Wide Association Study in Korean Men. *Clin Nutr Res*. 2020; 9(2):134–44. <https://doi.org/10.7762/cnr.2020.9.2.134> PMID: 32395443
44. Sunny SK, Zhang H, Relton CL, Ring S, Kadalayil L, Mzayek F, et al. Sex-specific longitudinal association of DNA methylation with lung function. *ERJ Open Res*. 2021; 7(3). <https://doi.org/10.1183/23120541.00127-2021> PMID: 34235211
45. Mukherjee N, Lockett GA, Merid SK, Melen E, Pershagen G, Holloway JW, et al. DNA methylation and genetic polymorphisms of the Leptin gene interact to influence lung function outcomes and asthma at 18 years of age. *Int J Mol Epidemiol Genet*. 2016; 7(1):1–17. PMID: 27186323
46. Zhang H, Tong X, Holloway JW, Rezwan FI, Lockett GA, Patil V, et al. The interplay of DNA methylation over time with Th2 pathway genetic variants on asthma risk and temporal asthma transition. *Clin Epigenetics*. 2014; 6(1):8. <https://doi.org/10.1186/1868-7083-6-8> PMID: 24735657
47. Munoz-Pizza DM, Villada-Canela M, Reyna MA, Texcalac-Sangrador JL, Osornio-Vargas AR. Air pollution and children's respiratory health: a scoping review of socioeconomic status as an effect modifier. *Int J Public Health*. 2020; 65(5):649–60. <https://doi.org/10.1007/s00038-020-01378-3> PMID: 32405779

48. Hajizadeh M, Nandi A. The socioeconomic gradient of secondhand smoke exposure in children: evidence from 26 low-income and middle-income countries. *Tob Control*. 2016; 25(e2):e146–e55. <https://doi.org/10.1136/tobaccocontrol-2015-052828> PMID: 27312823
49. Martinez CH, Mannino DM, Curtis JL, Han MK, Diaz AA. Socioeconomic Characteristics Are Major Contributors to Ethnic Differences in Health Status in Obstructive Lung Disease: An Analysis of the National Health and Nutrition Examination Survey 2007–2010. *Chest*. 2015; 148(1):151–8. <https://doi.org/10.1378/chest.14-1814> PMID: 25633478
50. Thakur N, Oh SS, Nguyen EA, Martin M, Roth LA, Galanter J, et al. Socioeconomic status and childhood asthma in urban minority youths. The GALA II and SAGE II studies. *Am J Respir Crit Care Med*. 2013; 188(10):1202–9. <https://doi.org/10.1164/rccm.201306-1016OC> PMID: 24050698
51. Oraka E, Iqbal S, Flanders WD, Brinker K, Garbe P. Racial and ethnic disparities in current asthma and emergency department visits: findings from the National Health Interview Survey, 2001–2010. *J Asthma*. 2013; 50(5):488–96. <https://doi.org/10.3109/02770903.2013.790417> PMID: 23544662
52. Keet CA, Matsui EC, McCormack MC, Peng RD. Urban residence, neighborhood poverty, race/ethnicity, and asthma morbidity among children on Medicaid. *J Allergy Clin Immunol*. 2017; 140(3):822–7. <https://doi.org/10.1016/j.jaci.2017.01.036> PMID: 28283418
53. Manrai AK, Funke BH, Rehm HL, Olesen MS, Maron BA, Szolovits P, et al. Genetic Misdiagnoses and the Potential for Health Disparities. *N Engl J Med*. 2016; 375(7):655–65. <https://doi.org/10.1056/NEJMsa1507092> PMID: 27532831
54. Landry LG, Ali N, Williams DR, Rehm HL, Bonham VL. Lack Of Diversity In Genomic Databases Is A Barrier To Translating Precision Medicine Research Into Practice. *Health Aff (Millwood)*. 2018; 37(5):780–5. <https://doi.org/10.1377/hlthaff.2017.1595> PMID: 29733732
55. Pongracic JA, Krouse RZ, Babineau DC, Zoratti EM, Cohen RT, Wood RA, et al. Distinguishing characteristics of difficult-to-control asthma in inner-city children and adolescents. *J Allergy Clin Immunol*. 2016; 138(4):1030–41. <https://doi.org/10.1016/j.jaci.2016.06.059> PMID: 27720017
56. Zoratti EM, Krouse RZ, Babineau DC, Pongracic JA, O'Connor GT, Wood RA, et al. Asthma phenotypes in inner-city children. *J Allergy Clin Immunol*. 2016; 138(4):1016–29. <https://doi.org/10.1016/j.jaci.2016.06.061> PMID: 27720016
57. Gern JE, Visness CM, Gergen PJ, Wood RA, Bloomberg GR, O'Connor GT, et al. The Urban Environment and Childhood Asthma (URECA) birth cohort study: design, methods, and study population. *BMC Pulm Med*. 2009; 9:17. <https://doi.org/10.1186/1471-2466-9-17> PMID: 19426496
58. Zhou X, Stephens M. Genome-wide efficient mixed-model analysis for association studies. *Nat Genet*. 2012; 44(7):821–4. <https://doi.org/10.1038/ng.2310> PMID: 22706312
59. Consortium EP, Moore JE, Purcaro MJ, Pratt HE, Epstein CB, Shores N, et al. Expanded encyclopaedias of DNA elements in the human and mouse genomes. *Nature*. 2020; 583(7818):699–710. <https://doi.org/10.1038/s41586-020-2493-4> PMID: 32728249
60. Ma M, Ru Y, Chuang LS, Hsu NY, Shi LS, Hakenberg J, et al. Disease-associated variants in different categories of disease located in distinct regulatory elements. *BMC Genomics*. 2015; 16 Suppl 8:S3. <https://doi.org/10.1186/1471-2164-16-S8-S3> PMID: 26110593
61. Boyle EA, Li Yi, Pritchard JK. An Expanded View of Complex Traits: From Polygenic to Omnigenic. *Cell*. 2017; 169(7):1177–86. <https://doi.org/10.1016/j.cell.2017.05.038> PMID: 28622505
62. Watanabe K, Stringer S, Frei O, Umicevic Mirkov M, de Leeuw C, Polderman TJC, et al. A global overview of pleiotropy and genetic architecture in complex traits. *Nat Genet*. 2019; 51(9):1339–48. <https://doi.org/10.1038/s41588-019-0481-0> PMID: 31427789
63. Schulz H, Ruppert AK, Herms S, Wolf C, Mirza-Schreiber N, Stegle O, et al. Genome-wide mapping of genetic determinants influencing DNA methylation and gene expression in human hippocampus. *Nat Commun*. 2017; 8(1):1511. <https://doi.org/10.1038/s41467-017-01818-4> PMID: 29142228
64. Huan T, Joehanes R, Song C, Peng F, Guo Y, Mendelson M, et al. Genome-wide identification of DNA methylation QTLs in whole blood highlights pathways for cardiovascular disease. *Nat Commun*. 2019; 10(1):4267. <https://doi.org/10.1038/s41467-019-12228-z> PMID: 31537805
65. Hannon E, Gorrie-Stone TJ, Smart MC, Burrage J, Hughes A, Bao Y, et al. Leveraging DNA-Methylation Quantitative-Trait Loci to Characterize the Relationship between Methylomic Variation, Gene Expression, and Complex Traits. *Am J Hum Genet*. 2018; 103(5):654–65. <https://doi.org/10.1016/j.ajhg.2018.09.007> PMID: 30401456
66. McKennan C, Naughton K, Stanhope C, Kattan M, O'Connor GT, Sandel MT, et al. Longitudinal data reveal strong genetic and weak non-genetic components of ethnicity-dependent blood DNA methylation levels. *Epigenetics*. 2021; 16(6):662–76. <https://doi.org/10.1080/15592294.2020.1817290> PMID: 32997571

67. Joubert BR, Felix JF, Yousefi P, Bakulski KM, Just AC, Breton C, et al. DNA Methylation in Newborns and Maternal Smoking in Pregnancy: Genome-wide Consortium Meta-analysis. *Am J Hum Genet.* 2016; 98(4):680–96. <https://doi.org/10.1016/j.ajhg.2016.02.019> PMID: 27040690
68. Sikdar S, Joehanes R, Joubert BR, Xu CJ, Vives-Usano M, Rezwan FI, et al. Comparison of smoking-related DNA methylation between newborns from prenatal exposure and adults from personal smoking. *Epigenomics.* 2019; 11(13):1487–500. <https://doi.org/10.2217/epi-2019-0066> PMID: 31536415
69. Nicolae DL, Gamazon E, Zhang W, Duan S, Dolan ME, Cox NJ. Trait-associated SNPs are more likely to be eQTLs: annotation to enhance discovery from GWAS. *PLoS Genet.* 2010; 6(4):e1000888. <https://doi.org/10.1371/journal.pgen.1000888> PMID: 20369019
70. Yao DW, O'Connor LJ, Price AL, Gusev A. Quantifying genetic effects on disease mediated by assayed gene expression levels. *Nat Genet.* 2020; 52(6):626–33. <https://doi.org/10.1038/s41588-020-0625-2> PMID: 32424349
71. Hormozdiari F, van de Bunt M, Segre AV, Li X, Joo JWW, Bilow M, et al. Colocalization of GWAS and eQTL Signals Detects Target Genes. *Am J Hum Genet.* 2016; 99(6):1245–60. <https://doi.org/10.1016/j.ajhg.2016.10.003> PMID: 27866706
72. Helling BA, Sobreira DR, Hansen GT, Sakabe NJ, Luo K, Billstrand C, et al. Altered transcriptional and chromatin responses to rhinovirus in bronchial epithelial cells from adults with asthma. *Commun Biol.* 2020; 3(1):678. <https://doi.org/10.1038/s42003-020-01411-4> PMID: 33188283
73. Samuels-Lev Y, O'Connor DJ, Bergamaschi D, Trigiante G, Hsieh JK, Zhong S, et al. ASPP proteins specifically stimulate the apoptotic function of p53. *Mol Cell.* 2001; 8(4):781–94. [https://doi.org/10.1016/s1097-2765\(01\)00367-7](https://doi.org/10.1016/s1097-2765(01)00367-7) PMID: 11684014
74. Aylon Y, Ofir-Rosenfeld Y, Yabuta N, Lapi E, Nojima H, Lu X, et al. The Lats2 tumor suppressor augments p53-mediated apoptosis by promoting the nuclear proapoptotic function of ASPP1. *Genes Dev.* 2010; 24(21):2420–9. <https://doi.org/10.1101/gad.1954410> PMID: 21041410
75. Wang Y, Godin-Heymann N, Dan Wang X, Bergamaschi D, Llanos S, Lu X. ASPP1 and ASPP2 bind active RAS, potentiate RAS signalling and enhance p53 activity in cancer cells. *Cell Death Differ.* 2013; 20(4):525–34. <https://doi.org/10.1038/cdd.2013.3> PMID: 23392125
76. Xue H, Li MX. MicroRNA-150 protects against cigarette smoke-induced lung inflammation and airway epithelial cell apoptosis through repressing p53: MicroRNA-150 in CS-induced lung inflammation. *Hum Exp Toxicol.* 2018; 37(9):920–8. <https://doi.org/10.1177/0960327117741749> PMID: 29205062
77. Xu F, Xu A, Guo Y, Bai Q, Wu X, Ji SP, et al. PM2.5 exposure induces alveolar epithelial cell apoptosis and causes emphysema through p53/Siva-1. *Eur Rev Med Pharmacol Sci.* 2020; 24(7):3943–50. https://doi.org/10.26355/eurrev_202004_20863 PMID: 32329870
78. Song Q, Zhou ZJ, Cai S, Chen Y, Chen P. Oxidative stress links the tumour suppressor p53 with cell apoptosis induced by cigarette smoke. *Int J Environ Health Res.* 2021. <https://doi.org/10.1080/09603123.2021.1910211> PMID: 33825597
79. Zhao K, Yu M, Zhu Y, Liu D, Wu Q, Hu Y. EGR-1/ASPP1 inter-regulatory loop promotes apoptosis by inhibiting cyto-protective autophagy. *Cell Death Dis.* 2017; 8(6):e2869. <https://doi.org/10.1038/cddis.2017.268> PMID: 28594407
80. Reynolds PR, Cosio MG, Hoidal JR. Cigarette smoke-induced Egr-1 upregulates proinflammatory cytokines in pulmonary epithelial cells. *Am J Respir Cell Mol Biol.* 2006; 35(3):314–9. <https://doi.org/10.1165/rcmb.2005-0428OC> PMID: 16601242
81. Chen ZH, Kim HP, Sciruba FC, Lee SJ, Feghali-Bostwick C, Stolz DB, et al. Egr-1 regulates autophagy in cigarette smoke-induced chronic obstructive pulmonary disease. *PLoS One.* 2008; 3(10):e3316. <https://doi.org/10.1371/journal.pone.0003316> PMID: 18830406
82. Shen N, Gong T, Wang JD, Meng FL, Qiao L, Yang RL, et al. Cigarette smoke-induced pulmonary inflammatory responses are mediated by EGR-1/GGPPS/MAPK signaling. *Am J Pathol.* 2011; 178(1):110–8. <https://doi.org/10.1016/j.ajpath.2010.11.016> PMID: 21224049
83. Wang SB, Zhang C, Xu XC, Xu F, Zhou JS, Wu YP, et al. Early growth response factor 1 is essential for cigarette smoke-induced MUC5AC expression in human bronchial epithelial cells. *Biochem Biophys Res Commun.* 2017; 490(2):147–54. <https://doi.org/10.1016/j.bbrc.2017.06.014> PMID: 28602698
84. Xu F, Cao J, Luo M, Che L, Li W, Ying S, et al. Early growth response gene 1 is essential for urban particulate matter-induced inflammation and mucus hyperproduction in airway epithelium. *Toxicol Lett.* 2018; 294:145–55. <https://doi.org/10.1016/j.toxlet.2018.05.003> PMID: 29787794
85. Golebski K, Gorenjak M, Kabesch M, Maitland-Van Der Zee A-H, Melén E, Potočnik U, et al. EGR-1 as a potential biomarker in asthma and proinflammatory responses in airway epithelium. *European Respiratory Journal.* 2021; 58(suppl 65):PA2041.

86. Wang A, Chiou J, Poirion OB, Buchanan J, Valdez MJ, Verheyden JM, et al. Single-cell multiomic profiling of human lungs reveals cell-type-specific and age-dynamic control of SARS-CoV2 host genes. *Elife*. 2020; 9. <https://doi.org/10.7554/eLife.62522> PMID: 33164753
87. Karlsson M, Zhang C, Mear L, Zhong W, Digre A, Katona B, et al. A single-cell type transcriptomics map of human tissues. *Sci Adv*. 2021; 7(31). <https://doi.org/10.1126/sciadv.abh2169> PMID: 34321199
88. Cheng Y, Luo W, Li Z, Cao M, Zhu Z, Han C, et al. CircRNA-012091/PPP1R13B-mediated Lung Fibrotic Response in Silicosis via Endoplasmic Reticulum Stress and Autophagy. *Am J Respir Cell Mol Biol*. 2019; 61(3):380–91. <https://doi.org/10.1165/rcmb.2019-0017OC> PMID: 30908929
89. Vigneron AM, Ludwig RL, Vousden KH. Cytoplasmic ASPP1 inhibits apoptosis through the control of YAP. *Genes Dev*. 2010; 24(21):2430–9. <https://doi.org/10.1101/gad.1954310> PMID: 21041411
90. Manfredi JJ. An identity crisis for a cancer gene: subcellular location determines ASPP1 function. *Cancer Cell*. 2010; 18(5):409–10. <https://doi.org/10.1016/j.ccr.2010.11.003> PMID: 21075306
91. Fogal V, Kartasheva NN, Trigiante G, Llanos S, Yap D, Vousden KH, et al. ASPP1 and ASPP2 are new transcriptional targets of E2F. *Cell Death Differ*. 2005; 12(4):369–76. <https://doi.org/10.1038/sj.cdd.4401562> PMID: 15731768
92. Zhou SJ, Li M, Zeng DX, Zhu ZM, Hu XW, Li YH, et al. Expression variations of connective tissue growth factor in pulmonary arteries from smokers with and without chronic obstructive pulmonary disease. *Sci Rep*. 2015; 5:8564. <https://doi.org/10.1038/srep08564> PMID: 25708588
93. Eguchi A, Nishizawa-Jotaki S, Tanabe H, Rahmutulla B, Watanabe M, Miyaso H, et al. An Altered DNA Methylation Status in the Human Umbilical Cord Is Correlated with Maternal Exposure to Polychlorinated Biphenyls. *Int J Environ Res Public Health*. 2019; 16(15). <https://doi.org/10.3390/ijerph16152786> PMID: 31382687
94. Pierce BL, Tong L, Argos M, Demanelis K, Jasmine F, Rakibuz-Zaman M, et al. Co-occurring expression and methylation QTLs allow detection of common causal variants and shared biological mechanisms. *Nat Commun*. 2018; 9(1):804. <https://doi.org/10.1038/s41467-018-03209-9> PMID: 29476079
95. Philibert RA, Sears RA, Powers LS, Nash E, Bair T, Gerke AK, et al. Coordinated DNA methylation and gene expression changes in smoker alveolar macrophages: specific effects on VEGF receptor 1 expression. *J Leukoc Biol*. 2012; 92(3):621–31. <https://doi.org/10.1189/jlb.1211632> PMID: 22427682
96. Guijo M, Ceballos-Chavez M, Gomez-Marin E, Basurto-Cayuela L, Reyes JC. Expression of TDRD9 in a subset of lung carcinomas by CpG island hypomethylation protects from DNA damage. *Oncotarget*. 2018; 9(11):9618–31. <https://doi.org/10.18632/oncotarget.22709> PMID: 29515758
97. Consortium GT. The Genotype-Tissue Expression (GTEx) project. *Nat Genet*. 2013; 45(6):580–5. <https://doi.org/10.1038/ng.2653> PMID: 23715323
98. Loh K, Modhukur V, Rajashekar B, Martens K, Magi R, Kolde R, et al. DNA methylome profiling of human tissues identifies global and tissue-specific methylation patterns. *Genome Biol*. 2014; 15(4):r54. <https://doi.org/10.1186/gb-2014-15-4-r54> PMID: 24690455
99. Wan J, Oliver VF, Wang G, Zhu H, Zack DJ, Merbs SL, et al. Characterization of tissue-specific differential DNA methylation suggests distinct modes of positive and negative gene expression regulation. *BMC Genomics*. 2015; 16:49. <https://doi.org/10.1186/s12864-015-1271-4> PMID: 25652663
100. den Dekker HT, Burrows K, Felix JF, Salas LA, Nedeljkovic I, Yao J, et al. Newborn DNA-methylation, childhood lung function, and the risks of asthma and COPD across the life course. *Eur Respir J*. 2019; 53(4). <https://doi.org/10.1183/13993003.01795-2018> PMID: 30765504
101. Imboden M, Wielscher M, Rezwan FI, Amaral AFS, Schaffner E, Jeong A, et al. Epigenome-wide association study of lung function level and its change. *Eur Respir J*. 2019; 54(1). <https://doi.org/10.1183/13993003.00457-2019> PMID: 31073081
102. Mukherjee N, Arathimos R, Chen S, Kheirkhah Rahimabad P, Han L, Zhang H, et al. DNA methylation at birth is associated with lung function development until age 26 years. *Eur Respir J*. 2021; 57(4).
103. Wang T, Wang W, Li W, Duan H, Xu C, Tian X, et al. Genome-wide DNA methylation analysis of pulmonary function in middle and old-aged Chinese monozygotic twins. *Respir Res*. 2021; 22(1):300. <https://doi.org/10.1186/s12931-021-01896-5> PMID: 34809630
104. Herrera-Luis E, Li A, Mak ACY, Perez-Garcia J, Elhawary JR, Oh SS, et al. Epigenome-wide association study of lung function in Latino children and youth with asthma. *Clin Epigenetics*. 2022; 14(1):9. <https://doi.org/10.1186/s13148-022-01227-5> PMID: 35033200
105. Cosin-Tomas M, Bustamante M, Sunyer J. Epigenetic association studies at birth and the origin of lung function development. *Eur Respir J*. 2021; 57(4). <https://doi.org/10.1183/13993003.00109-2021> PMID: 33858853
106. Yang IV, Lozupone CA, Schwartz DA. The environment, epigenome, and asthma. *J Allergy Clin Immunol*. 2017; 140(1):14–23. <https://doi.org/10.1016/j.jaci.2017.05.011> PMID: 28673400

107. Lin PI, Shu H, Mersha TB. Comparing DNA methylation profiles across different tissues associated with the diagnosis of pediatric asthma. *Sci Rep.* 2020; 10(1):151. <https://doi.org/10.1038/s41598-019-56310-4> PMID: 31932625
108. Richmond RC, Davey Smith G. Mendelian Randomization: Concepts and Scope. *Cold Spring Harb Perspect Med.* 2022; 12(1). <https://doi.org/10.1101/cshperspect.a040501> PMID: 34426474
109. Robins JM, Greenland S. Identifiability and exchangeability for direct and indirect effects. *Epidemiology.* 1992; 3(2):143–55. <https://doi.org/10.1097/00001648-199203000-00013> PMID: 1576220
110. Li YF, Gilliland FD, Berhane K, McConnell R, Gauderman WJ, Rappaport EB, et al. Effects of in utero and environmental tobacco smoke exposure on lung function in boys and girls with and without asthma. *Am J Respir Crit Care Med.* 2000; 162(6):2097–104. <https://doi.org/10.1164/ajrccm.162.6.2004178> PMID: 11112121
111. Gilliland FD, Berhane K, Li YF, Rappaport EB, Peters JM. Effects of early onset asthma and in utero exposure to maternal smoking on childhood lung function. *Am J Respir Crit Care Med.* 2003; 167(6):917–24. <https://doi.org/10.1164/rccm.200206-616OC> PMID: 12480608
112. Schultz ES, Litorjua AA, Melen E. Effects of Long-Term Exposure to Traffic-Related Air Pollution on Lung Function in Children. *Curr Allergy Asthma Rep.* 2017; 17(6):41. <https://doi.org/10.1007/s11882-017-0709-y> PMID: 28551888
113. Kreiner-Moller E, Bisgaard H, Bonnelykke K. Prenatal and postnatal genetic influence on lung function development. *J Allergy Clin Immunol.* 2014; 134(5):1036–42 e15. <https://doi.org/10.1016/j.jaci.2014.04.003> PMID: 24857373
114. Lee EY, Mak ACY, Hu D, Sajuthi S, White MJ, Keys KL, et al. Whole-Genome Sequencing Identifies Novel Functional Loci Associated with Lung Function in Puerto Rican Youth. *Am J Respir Crit Care Med.* 2020; 202(7):962–72. <https://doi.org/10.1164/rccm.202002-0351OC> PMID: 32459537
115. Goddard PC, Keys KL, Mak ACY, Lee EY, Liu AK, Samedy-Bates LA, et al. Integrative genomic analysis in African American children with asthma finds three novel loci associated with lung function. *Genet Epidemiol.* 2021; 45(2):190–208. <https://doi.org/10.1002/gepi.22365> PMID: 32989782
116. Akenroye AT, Brunetti T, Romero K, Daya M, Kanchan K, Shankar G, et al. Genome-wide association study of asthma, total IgE, and lung function in a cohort of Peruvian children. *J Allergy Clin Immunol.* 2021; 148(6):1493–504. <https://doi.org/10.1016/j.jaci.2021.02.035> PMID: 33713768
117. Imboden M, Bouzigon E, Curjuric I, Ramasamy A, Kumar A, Hancock DB, et al. Genome-wide association study of lung function decline in adults with and without asthma. *J Allergy Clin Immunol.* 2012; 129(5):1218–28. <https://doi.org/10.1016/j.jaci.2012.01.074> PMID: 22424883
118. Aschard H, Vilhjalmsdottir BJ, Joshi AD, Price AL, Kraft P. Adjusting for heritable covariates can bias effect estimates in genome-wide association studies. *Am J Hum Genet.* 2015; 96(2):329–39. <https://doi.org/10.1016/j.ajhg.2014.12.021> PMID: 25640676
119. Jones MJ, Goodman SJ, Kobor MS. DNA methylation and healthy human aging. *Aging Cell.* 2015; 14(6):924–32. <https://doi.org/10.1111/acer.12349> PMID: 25913071
120. Ambatipudi S, Cuenin C, Hernandez-Vargas H, Ghantous A, Le Calvez-Kelm F, Kaaks R, et al. Tobacco smoking-associated genome-wide DNA methylation changes in the EPIC study. *Epigenomics.* 2016; 8(5):599–618. <https://doi.org/10.2217/epi-2016-0001> PMID: 26864933
121. Tommasi S, Zheng A, Besaratinia A. Exposure of mice to secondhand smoke elicits both transient and long-lasting transcriptional changes in cancer-related functional networks. *Int J Cancer.* 2015; 136(10):2253–63. <https://doi.org/10.1002/ijc.29284> PMID: 25346222
122. Sridhar S, Schembri F, Zeskind J, Shah V, Gustafson AM, Steiling K, et al. Smoking-induced gene expression changes in the bronchial airway are reflected in nasal and buccal epithelium. *BMC Genomics.* 2008; 9:259. <https://doi.org/10.1186/1471-2164-9-259> PMID: 18513428
123. Zhang X, Sebastiani P, Liu G, Schembri F, Zhang X, Dumas YM, et al. Similarities and differences between smoking-related gene expression in nasal and bronchial epithelium. *Physiol Genomics.* 2010; 41(1):1–8. <https://doi.org/10.1152/physiolgenomics.00167.2009> PMID: 19952278
124. Brugha R, Lowe R, Henderson AJ, Holloway JW, Rakyan V, Wozniak E, et al. DNA methylation profiles between airway epithelium and proxy tissues in children. *Acta Paediatr.* 2017; 106(12):2011–6. <https://doi.org/10.1111/apa.14027> PMID: 28833606
125. Imkamp K, Berg M, Vermeulen CJ, Heijink IH, Guryev V, Kerstjens HAM, et al. Nasal epithelium as a proxy for bronchial epithelium for smoking-induced gene expression and expression Quantitative Trait Loci. *J Allergy Clin Immunol.* 2018; 142(1):314–7 e15. <https://doi.org/10.1016/j.jaci.2018.01.047> PMID: 29522853
126. Kicic A, de Jong E, Ling KM, Nichol K, Anderson D, Wark PAB, et al. Assessing the unified airway hypothesis in children via transcriptional profiling of the airway epithelium. *J Allergy Clin Immunol.* 2020; 145(6):1562–73. <https://doi.org/10.1016/j.jaci.2020.02.018> PMID: 32113981

127. Bergougnoux A, Claustres M, De Sario A. Nasal epithelial cells: a tool to study DNA methylation in airway diseases. *Epigenomics*. 2015; 7(1):119–26. <https://doi.org/10.2217/epi.14.65> PMID: 25687471
128. Stoffel B, Sorkness C, Pech C. Use of a Single, Independent IRB: Case Study of an NIH Funded Consortium. *Contemp Clin Trials Commun*. 2017; 8:114–21. <https://doi.org/10.1016/j.conctc.2017.09.001> PMID: 29546249
129. Gergen PJ, Teach SJ, Trogias A, Busse WW. Reducing Exacerbations in the Inner City: Lessons from the Inner-City Asthma Consortium (ICAC). *J Allergy Clin Immunol Pract*. 2016; 4(1):22–6. <https://doi.org/10.1016/j.jaip.2015.07.024> PMID: 26589178
130. O'Connor GT, Lynch SV, Bloomberg GR, Kattan M, Wood RA, Gergen PJ, et al. Early-life home environment and risk of asthma among inner-city children. *J Allergy Clin Immunol*. 2018; 141(4):1468–75. <https://doi.org/10.1016/j.jaci.2017.06.040> PMID: 28939248
131. Quanjer PH, Stanojevic S, Cole TJ, Baur X, Hall GL, Culver BH, et al. Multi-ethnic reference values for spirometry for the 3-95-yr age range: the global lung function 2012 equations. *Eur Respir J*. 2012; 40(6):1324–43. <https://doi.org/10.1183/09031936.00080312> PMID: 22743675
132. Bernert JT, Harmon TL, Sosnoff CS, McGuffey JE. Use of cotinine immunoassay test strips for pre-classifying urine samples from smokers and nonsmokers prior to analysis by LC-MS-MS. *J Anal Toxicol*. 2005; 29(8):814–8. <https://doi.org/10.1093/jat/29.8.814> PMID: 16374940
133. Regier AA, Farjoun Y, Larson DE, Krasheninina O, Kang HM, Howrigan DP, et al. Functional equivalence of genome sequencing analysis pipelines enables harmonized variant calling across human genetics projects. *Nat Commun*. 2018; 9(1):4038. <https://doi.org/10.1038/s41467-018-06159-4> PMID: 30279509
134. Kowalski MH, Qian H, Hou Z, Rosen JD, Tapia AL, Shan Y, et al. Use of >100,000 NHLBI Trans-Omics for Precision Medicine (TOPMed) Consortium whole genome sequences improves imputation quality and detection of rare variant associations in admixed African and Hispanic/Latino populations. *PLoS Genet*. 2019; 15(12):e1008500.
135. Zhang F, Flickinger M, Taliun SAG, In PPGC, Abecasis GR, Scott LJ, et al. Ancestry-agnostic estimation of DNA sample contamination from sequence reads. *Genome Res*. 2020; 30(2):185–94. <https://doi.org/10.1101/gr.246934.118> PMID: 31980570
136. Chang CC, Chow CC, Tellier LC, Vattikuti S, Purcell SM, Lee JJ. Second-generation PLINK: rising to the challenge of larger and richer datasets. *Gigascience*. 2015; 4:7. <https://doi.org/10.1186/s13742-015-0047-8> PMID: 25722852
137. McKennan C, Naughton K, Stanhope C, Kattan M, O'Connor GT, Sandel MT, et al. Longitudinal data reveal strong genetic and weak non-genetic components of ethnicity-dependent blood DNA methylation levels. *Epigenetics*. 2020. <https://doi.org/10.1080/15592294.2020.1817290> PMID: 32997571
138. Jun G, Flickinger M, Hetrick KN, Romm JM, Doheny KF, Abecasis GR, et al. Detecting and estimating contamination of human DNA samples in sequencing and array-based genotype data. *Am J Hum Genet*. 2012; 91(5):839–48. <https://doi.org/10.1016/j.ajhg.2012.09.004> PMID: 23103226
139. Hao W, Storey JD. Extending Tests of Hardy-Weinberg Equilibrium to Structured Populations. *Genetics*. 2019; 213(3):759–70. <https://doi.org/10.1534/genetics.119.302370> PMID: 31537622
140. Danecek P, Auton A, Abecasis G, Albers CA, Banks E, DePristo MA, et al. The variant call format and VCFtools. *Bioinformatics*. 2011; 27(15):2156–8. <https://doi.org/10.1093/bioinformatics/btr330> PMID: 21653522
141. Danecek P, Bonfield JK, Liddle J, Marshall J, Ohan V, Pollard MO, et al. Twelve years of SAMtools and BCFtools. *Gigascience*. 2021; 10(2). <https://doi.org/10.1093/gigascience/giab008> PMID: 33590861
142. Genomes Project C, Auton A, Brooks LD, Durbin RM, Garrison EP, Kang HM, et al. A global reference for human genetic variation. *Nature*. 2015; 526(7571):68–74. <https://doi.org/10.1038/nature15393> PMID: 26432245
143. Bergstrom A, McCarthy SA, Hui R, Almarri MA, Ayub Q, Danecek P, et al. Insights into human genetic variation and population history from 929 diverse genomes. *Science*. 2020; 367(6484). <https://doi.org/10.1126/science.aay5012> PMID: 32193295
144. Alexander DH, Novembre J, Lange K. Fast model-based estimation of ancestry in unrelated individuals. *Genome Res*. 2009; 19(9):1655–64. <https://doi.org/10.1101/gr.094052.109> PMID: 19648217
145. Conomos MP, Miller MB, Thornton TA. Robust inference of population structure for ancestry prediction and correction of stratification in the presence of relatedness. *Genet Epidemiol*. 2015; 39(4):276–93. <https://doi.org/10.1002/gepi.21896> PMID: 25810074
146. Conomos MP, Reiner AP, Weir BS, Thornton TA. Model-free Estimation of Recent Genetic Relatedness. *Am J Hum Genet*. 2016; 98(1):127–48. <https://doi.org/10.1016/j.ajhg.2015.11.022> PMID: 26748516

147. Manichaikul A, Mychaleckyj JC, Rich SS, Daly K, Sale M, Chen WM. Robust relationship inference in genome-wide association studies. *Bioinformatics*. 2010; 26(22):2867–73. <https://doi.org/10.1093/bioinformatics/btq559> PMID: 20926424
148. Shringarpure SS, Bustamante CD, Lange K, Alexander DH. Efficient analysis of large datasets and sex bias with ADMIXTURE. *BMC Bioinformatics*. 2016; 17:218. <https://doi.org/10.1186/s12859-016-1082-x> PMID: 27216439
149. Sofer T, Zheng X, Gogarten SM, Laurie CA, Grinde K, Shaffer JR, et al. A fully adjusted two-stage procedure for rank-normalization in genetic association studies. *Genet Epidemiol*. 2019; 43(3):263–75. <https://doi.org/10.1002/gepi.22188> PMID: 30653739
150. McCaw ZR, Lane JM, Saxena R, Redline S, Lin X. Operating characteristics of the rank-based inverse normal transformation for quantitative trait analysis in genome-wide association studies. *Biometrics*. 2020; 76(4):1262–72. <https://doi.org/10.1111/biom.13214> PMID: 31883270
151. Wang G, Sarkar A, Carbonetto P, Stephens M. A simple new approach to variable selection in regression, with application to genetic fine mapping. *Journal of the Royal Statistical Society: Series B (Statistical Methodology)*. 2020; 82(5):1273–300.
152. Shabalin AA. Matrix eQTL: ultra fast eQTL analysis via large matrix operations. *Bioinformatics*. 2012; 28(10):1353–8. <https://doi.org/10.1093/bioinformatics/bts163> PMID: 22492648
153. McKennan C, Nicolae D. Accounting for unobserved covariates with varying degrees of estimability in high-dimensional biological data. *Biometrika*. 2019; 106(4):823–40. <https://doi.org/10.1093/biomet/asz037> PMID: 31754283
154. Zhang D. A Coefficient of Determination for Generalized Linear Models. *The American Statistician*. 2017; 71(4):310–6.
155. Fox J, Kleiber C, Zeileis A. *ivreg: Two-Stage Least-Squares Regression with Diagnostics*. <https://john-d-fox.github.io/ivreg/2021>.
156. Burgess S, Small DS, Thompson SG. A review of instrumental variable estimators for Mendelian randomization. *Stat Methods Med Res*. 2017; 26(5):2333–55. <https://doi.org/10.1177/0962280215597579> PMID: 26282889
157. Burgess S, Thompson SG. Use of allele scores as instrumental variables for Mendelian randomization. *International Journal of Epidemiology*. 2013; 42(4):1134–44. <https://doi.org/10.1093/ije/dyt093> PMID: 24062299
158. Alfons A, Ateş NY, Groenen PJF. A Robust Bootstrap Test for Mediation Analysis. *Organizational Research Methods*. 0(0):1094428121999096.
159. Dobin A, Davis CA, Schlesinger F, Drenkow J, Zaleski C, Jha S, et al. STAR: ultrafast universal RNA-seq aligner. *Bioinformatics*. 2013; 29(1):15–21. <https://doi.org/10.1093/bioinformatics/bts635> PMID: 23104886
160. Law CW, Chen Y, Shi W, Smyth GK. voom: Precision weights unlock linear model analysis tools for RNA-seq read counts. *Genome Biol*. 2014; 15(2):R29. <https://doi.org/10.1186/gb-2014-15-2-r29> PMID: 24485249
161. Ritchie ME, Phipson B, Wu D, Hu Y, Law CW, Shi W, et al. limma powers differential expression analyses for RNA-sequencing and microarray studies. *Nucleic Acids Res*. 2015; 43(7):e47. <https://doi.org/10.1093/nar/gkv007> PMID: 25605792
162. Jager R, Migliorini G, Henrion M, Kandaswamy R, Speedy HE, Heindl A, et al. Capture Hi-C identifies the chromatin interactome of colorectal cancer risk loci. *Nat Commun*. 2015; 6:6178. <https://doi.org/10.1038/ncomms7178> PMID: 25695508
163. Mifsud B, Tavares-Cadete F, Young AN, Sugar R, Schoenfelder S, Ferreira L, et al. Mapping long-range promoter contacts in human cells with high-resolution capture Hi-C. *Nat Genet*. 2015; 47(6):598–606. <https://doi.org/10.1038/ng.3286> PMID: 25938943
164. Montefiori LE, Sobreira DR, Sakabe NJ, Aneas I, Joslin AC, Hansen GT, et al. A promoter interaction map for cardiovascular disease genetics. *Elife*. 2018; 7. <https://doi.org/10.7554/eLife.35788> PMID: 29988018
165. Cairns J, Freire-Pritchett P, Wingett SW, Varnai C, Dimond A, Plagnol V, et al. CHiCAGO: robust detection of DNA looping interactions in Capture Hi-C data. *Genome Biol*. 2016; 17(1):127. <https://doi.org/10.1186/s13059-016-0992-2> PMID: 27306882